

STUDIES IN THE FIELD OF CHEMISTRY OF NITRO COMPOUNDS (TO 100TH BIRTHDAY ANNIVERSARY OF S. S. NOVIKOV)

Primary Steps of the Mechanism of Gas-Phase Monomolecular Decomposition of Nitropropenes, According to Results of Quantum-Chemical Calculations (Review)

A. G. Shamov, E. V. Nikolaeva, and G. M. Khrapkovskii

Kazan State University of Technology, Kazan, Tatarstan, Russia

Received April 29, 2009

Abstract—The mechanisms of gas-phase monomolecular decomposition of *cis*- and *trans*-nitropropenes, 2-nitro-1-propene, and 2-methyl-1-nitro-1-propene were examined by DFT B3LYP/6-31G(d) calculations using GAUSSIAN'98 program package. The most probable pathway of thermal decomposition of these compounds involves formation in the primary step of four-membered cyclic intermediates, substituted oxazetes. For *cis*-nitropropene and 2-methyl-1-nitro-1-propene, the mechanism whose primary step is 1,5-sigmatropic hydrogen shift from the CH₃ group to the NO₂ group is principally possible.

DOI: 10.1134/S1070427209100024

Much attention has been given recently to studying the structure and reactivity of nitroolefins, as they are promising explosives. Therefore, theoretical and experimental studies on the synthesis and decomposition of nitroethylene and its substituted derivatives are performed in Russia and other countries [1–5].

It was found previously [5–8] that thermal monomolecular decomposition of nitroethylene (**I**) occurs

via formation in the limiting step of 4*H*-1,2-oxazete 2-oxide, rather than via elimination of HNO₂ as suggested in experimental studies (Table 1) [9]. The suggested mechanism of thermal decomposition of the simplest representative of nitroolefins is consistent with the available experimental and theoretical data [9–13]. In particular, the activation energy of its primary step is close to the experimental estimate (191.9 kJ mol^{–1} [9]).

Table 1. Activation energies of primary events of thermal monomolecular decomposition of nitroethylene

Process	ΔH_{298}^\ddagger , kJ mol ^{–1}		
	B3LYP		QCISD(T)
	6-31G(d)	6-311 ⁺⁺ G(df,p)	6-31G(d)
Cleavage of CN bond	281.2	268.4	289.5
Elimination of HO–N=O	243.4	223.9	253.2
Nitro–nitrite rearrangement	241.5	237.4	244.5
1,3- <i>H</i> -Sigmatropic shift to <i>aci</i> form	257.6	249.2	274.8
1,4- <i>H</i> -Sigmatropic shift to <i>aci</i> form	300.4	280.2	–
Formation of 4 <i>H</i> -1,2-oxazete 2-oxide	201.3	203.9	216.5

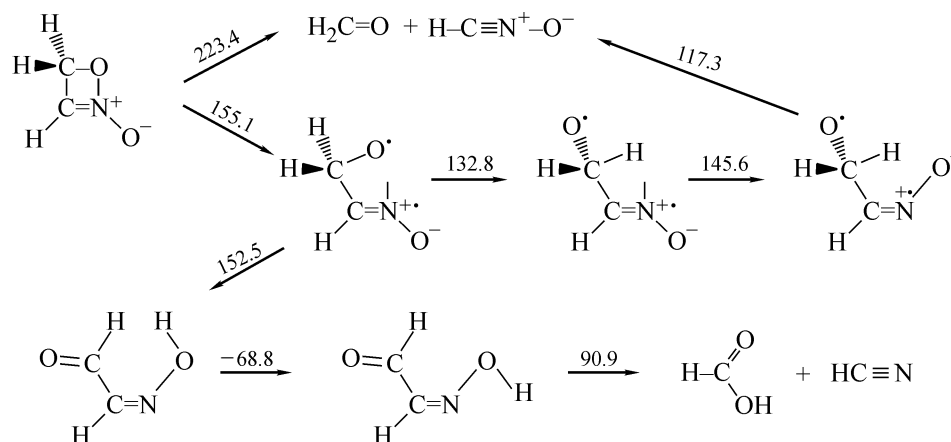


Fig. 1. Scheme of decomposition of 4H-1,2-oxazete 2-oxide [B3LYP/6-311++G(df,p)]. Figures over arrows denote the relative enthalpy of formation of the transition state corresponding to the given process (kJ mol⁻¹). The enthalpy of formation of nitroethylene is taken as zero.

Further progress of the reaction involves formation of a singlet biradical intermediate which either decomposes into formaldehyde and nitrile oxide after a series of conformational transitions or rearranges into aldoxime with its subsequent decomposition to hydrogen cyanide and formic acid (Fig. 1).

Taking into account steadily growing interest in thermal decomposition of substituted nitroethylenes, we examined the effect of substituents on the mechanism of gas-phase monomolecular decomposition of nitroolefins. This paper deals with primary steps of the mechanism of thermal decomposition of isomeric and substituted nitropropenes, namely, *cis*-nitropropene (**1a**), *trans*-nitropropene (**1'a**), 2-nitro-1-propene (**1''a**), and 2-methyl-1-nitro-1-propene (**1b**).

All the calculations were performed by the B3LYP/6-31G(d) method using GAUSSIAN'98 program package [14].

The procedure was described in detail in [8]. All the solutions were checked for stability [15] toward fluctuations imposed on the wavefunction using the Stable procedure in the GAUSSIAN'98 program, with the aim to make sure that the solutions found correspond to the

minimal energy.

Radical decomposition. In contrast to nitroalkanes and nitroarenes, regular trends in thermal decomposition of nitroalkenes are insufficiently understood. Only data on the kinetics of gas-phase decomposition of nitroethylene and several its simplest derivatives are available from the literature. Because nitroolefins under the experimental conditions at relatively low temperatures decompose by various nonradical mechanisms, kinetic estimations of the bond dissociation energies for this class of nitro compounds are lacking. Quantum-chemical estimations of the dissociation energy of the CN bond in nitroethylene and certain its aminonitro derivatives are made in [1, 4, 5]. Based on these results and on the data obtained for nitroalkanes [16] and nitroarenes [17], it can be concluded that the strength of the CN bond monotonically increases in the order nitromethane < nitroethylene < nitrobenzene. It should be noted that the strength and length of this bond in nitrobenzene and nitroethylene differ insignificantly (292 and 281 kJ mol⁻¹; 147.2 and 146.5 pm, respectively [5, 17]) (Scheme 1).

Of considerable interest are data on the CN bond strength in nitropropenes (Table 2).

Scheme 1.

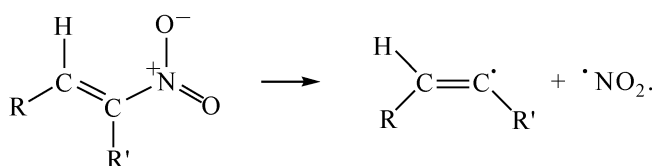


Table 2. Activation enthalpies ΔH^\ddagger of radical decomposition and enthalpies of formation of compounds, ΔH_f and radicals, $\Delta H_f^{(R)}$, formed in cleavage of CN bond in nitroolefins

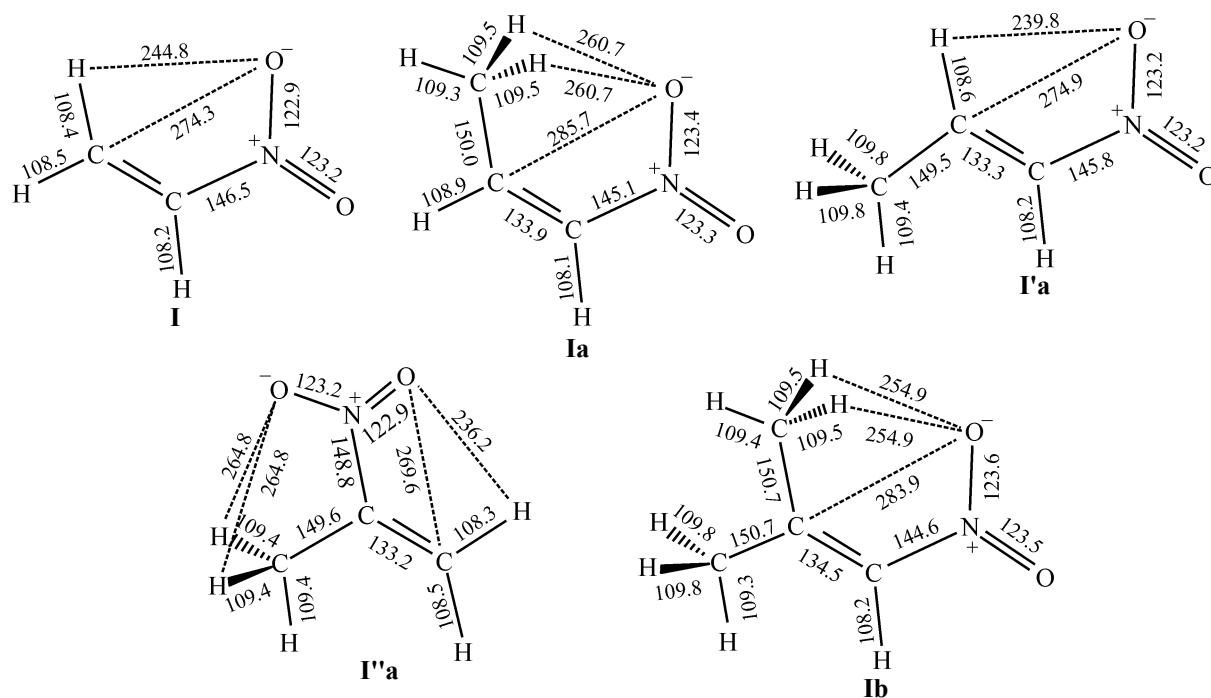
Compound	ΔH^\ddagger (298 K), kJ mol ⁻¹	ΔH_f (298 K), kJ mol ⁻¹	R [•]	$\Delta H_f^{(R)}$ (298 K), kJ mol ⁻¹
Nitroethylene	281.2	46.7	C ₂ H ₃ [•]	305.0 (299±5) ^a
<i>cis</i> -Nitropropene	281.1	20.5	<i>cis</i> -C ₃ H ₅ [•]	278.6 (246.9±21) ^b
-Nitropropene	291.8	9.8	<i>trans</i> -C ₃ H ₅ [•]	279.9
2-Nitro-1-propene	270.7	10.0	CH ₃ C [•] CH ₂	257.8
2-Methyl-1-nitro-1-propene	288.4	-13.0	C ₄ H ₇ [•]	252.4

^a Experimental value [18].^b Quantum-chemical estimation by nonempirical methods [19].

Analysis of trends in variation of the enthalpies of formation of compounds and radicals shows that the variation of the CN bond dissociation energy in *cis*- and *trans*-nitropropenes is chiefly determined by differences in the enthalpy of formation of the starting compounds, because the enthalpies of formation of the radicals formed by radical elimination of the nitro group are fairly close (the observed differences do not exceed 1.3 kJ mol⁻¹).

In turn, the differences in the enthalpies of formation

of the starting compounds can be attributed to specific features of their geometric and electronic structure (Figs. 2, 3). Lower enthalpy of formation of the *trans* isomer is apparently due to more favorable conditions for the formation of an intramolecular hydrogen bond, additionally stabilizing its structure. At the same time, in the *cis* isomer one can expect relatively strong repulsion of the oxygen atom of the nitro group and carbon atom of the methyl group, both bearing significant negative charges (Fig. 3).

**Fig. 2.** Geometric parameters of nitroethylene (I), *cis*-nitropropene (Ia), *trans*-nitropropene (I'a), 2-nitro-1-propene (I''a), and 2-methyl-1-nitro-1-propene (Ib), calculated by the B3LYP/6-31G(d) method. Bond lengths are given in picometers; the same for Figs. 4, 6, 8, 10–12, 14, 17, 18, 20, and 21.

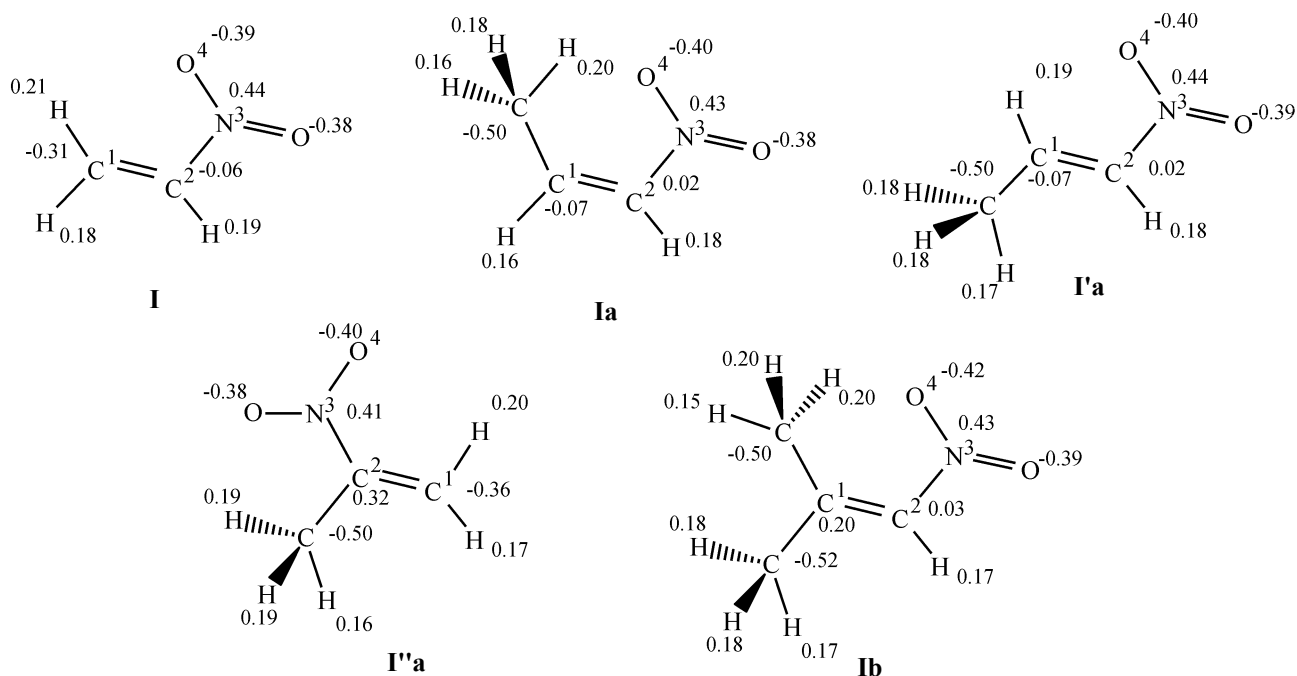


Fig. 3. Total charges (au) on atoms of nitroethylene (**I**), *cis*-nitropropene (**Ia**), *trans*-nitropropene (**Ia'**), 2-nitro-1-propene (**I'a**), and 2-methyl-1-nitro-1-propene (**Ib**), calculated by the B3LYP/6-31G(d) method.

A decrease in the activation enthalpy ΔH^\ddagger of the cleavage of the CN bond in 2-nitro-1-propene relative to compounds **I**, **Ia**, and **I'a** is apparently due to steric strain caused by repulsion of nonbonded atoms (primarily by the already noted repulsion of the methyl carbon atom and oxygen atom of the nitro group). The increased CN bond length in **I'a** relative to the other compounds under consideration (Fig. 2) is also a manifestation of the steric hindrance.

In 2-methyl-1-nitro-1-propene, ΔH^\ddagger of cleavage of the CN bond, according to the calculation results, exceeds by more than 7 kJ mol⁻¹ the values obtained for nitroethylene and *cis*-nitropropene and is by approximately 3 kJ mol⁻¹ lower than the value obtained for *trans*-nitropropene. Apparently, in this case the effects manifested for **Ia** and **I'a** compensate each other. Owing to the repulsion of the CH₃ groups from each other, which is confirmed by a certain increase in the CC bond length in **Ib** (Fig. 2) relative to the other compounds under consideration, the distance

between the hydrogen atoms of the methyl group in the *cis* position to the nitro group and the oxygen atom of the NO₂ group decreases. This fact results in strengthening of the CN bond in 2-methyl-1-nitro-1-propene relative to nitroethylene and *cis*-nitropropene. However, the presence of the CH₃ and NO₂ groups with the negatively charged C and N atoms in the *cis* position (Fig. 3) leads to the repulsion between these groups and, as a consequence, to a decrease in ΔH^\ddagger of cleavage of the CN bond in **Ib** relative to *trans*-nitropropene.

Elimination of HNO₂. Nazin et al. examined the kinetics of gas-phase decomposition [20] of α -nitroolefins and suggested that the primary event of their gas-phase monomolecular decomposition is associated with the elimination of HNO₂ via a five-membered transition state (Scheme 2).

This assumption was based on close experimental values of the activation energy and preexponential fac-

Scheme 2.

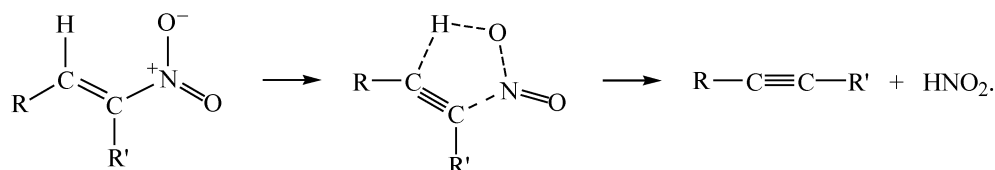


Table 3. Activation enthalpies ΔH^\ddagger and entropies ΔS^\ddagger , enthalpies of formation of the complexes of products ΔH_f^c , total enthalpies of formation of products $\Sigma \Delta H_f^{pr}$, and dipole moments of the reactants, μ_D^0 , transition states, μ_D^\ddagger , and complexes of products, μ_D^c , for HNO_2 elimination from certain nitroolefins

Compound	$\Delta H_{(298\text{ K})}^\ddagger$, kJ mol ⁻¹	$\Delta S_{(298\text{ K})}^\ddagger$, J mol ⁻¹ K ⁻¹	$\Sigma\Delta H_f^c$ (298 K)	$\Sigma\Delta H_f^{\text{pf}}$ (298 K)	μ_D^0	μ_D^\ddagger	μ_D^c
			kJ mol ⁻¹		D		
Nitriethylene	243.4	4.1	193.1	207.3	4.25	3.10	3.02
<i>trans</i> -Nitropropene	248.2	12.9	139.3	158.2	4.71	3.69	3.69
2-Nitro-1-propene (process 2)	223.8	12.2	139.3	158.2	3.88	4.10	3.09
2-Nitro-1-propene (process 3)	217.3	2.2	131.9	145.4	3.88	3.39	3.00

tors for the thermal decomposition of structurally related nitroalkanes and nitroalkenes. However, in contrast to nitroalkanes for which the molecular mechanism of the HNO_2 elimination is confirmed by detailed data on the product composition, in the case of nitroolefins reliable data on the product composition are lacking, and this mechanism is hypothetical. Nevertheless, this assumption was used for a relatively long time in discussion of experimental results and was not in doubt [9].

In [5–7] we showed for the first time that the barrier to elimination of nitrous acid from compound **I** [223.9 kJ mol^{-1} , according to B3LYP/6-311++G(df,p) calculations] exceeds the experimentally measured activation energy of the gas-phase decomposition (191.9 kJ mol^{-1} [9, 20, 21]). Considerable (up to 33.5–50.2 kJ mol^{-1} with different basis sets) differences between these quantities exceed the possible error of the quantum-chemical estimation of the reaction barrier. Therefore, the calculation results do not confirm the conclusion made in the experimental studies [9, 20, 21] that the gas-phase decomposition of nitroethylene occurs by the mechanism of HNO_2 elimination.

We determined the activation enthalpies and entropies of this reaction for certain methyl-substituted nitroethylenes (Table 3).

The data obtained show that, for *trans*-nitropropene, the activation enthalpy of reaction (2) exceeds the barrier of the related process for **I** by only 5 kJ mol^{-1} . However, the activation entropy for *trans*-nitropropene is three times higher than for nitroethylene. Therefore, the transition state of reaction (2) for compound **I'a** is presumably looser than for **I**. Indeed, analysis of the variation of the reaction center parameters (Figs. 2, 4) shows that the CN, NO, and CH bond lengths in *trans*-nitropropene

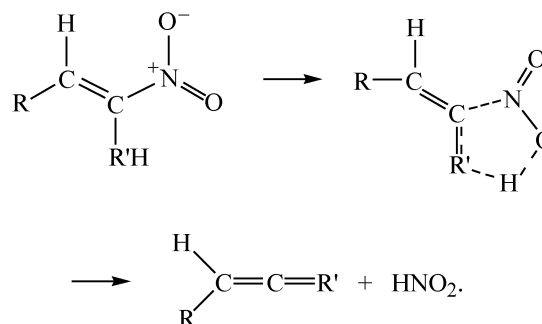
increase in the course of the reaction by 69.4, 5.7, and 34.5 pm, respectively, and the HO bond length decreases by 119.2 pm. In nitroethylene $\Delta \text{CN} = 64.2$, $\Delta \text{NO} = 4.9$, $\Delta \text{CH} = 36.5$, and $\Delta \text{HO} = -126.5$ pm.

For 2-nitro-1-propene (**I'a**), two pathways of HNO_2 elimination are possible.

The first pathway follows scheme (2) (transition state [**I'a**] ‡ is shown in Fig. 4). Its activation enthalpy (Table 3) is lower by 20 kJ mol^{-1} than that of the related reaction of nitroethylene. In the course of reaction (2) with **I'a**, the bond lengths change as follows: $\Delta \text{CN} = 77.9$, $\Delta \text{NO} = 6.0$, $\Delta \text{CH} = 20.6$, and $\Delta \text{HO} = -113.1$ pm. As seen from these data, in elimination of HNO_2 from **I'a** along pathway (2), only the CN bond length changes significantly, and the other bond lengths increase (CH, NO) or decrease (HO) less significantly than in nitroethylene and *trans*-nitropropene.

The second mechanism of HNO_2 elimination from 2-nitro-1-propene is possible owing to the presence of a hydrogen-containing substituent at the carbon atom bonded to the nitro group. It can be described by Scheme 3.

Scheme 3.



The structure of the transition state of this process is shown in Fig. 4. The activation enthalpy of reaction (3) compared to reaction (2) decreases for **I''a** by 5 kJ mol⁻¹ more (Table 3). This may be due to smaller changes in the CN bond length in the transition state ($\Delta\text{CN} = 71.7$ pm). In the process, the HO bond length decreases considerably ($\Delta\text{HO} = -142.4$ pm). The other bond lengths change to approximately the same extent as in the other compounds under consideration: $\Delta\text{NO} = 5.8$ and $\Delta\text{CH} = 32.4$ pm (Figs. 2, 4).

Discussions of the effect of substituents on the activation energy of gas-phase elimination of HNO₂ from aliphatic nitro compounds, performed in experimental studies, are based on the concept of a polar transition state [9, 22]. Quantum-chemical calculations, however, do not confirm this assumption (Fig. 5, Table 3). In the reactions of nitroethylene, *trans*-nitropropene, and 2-nitro-1-propene [reaction (3)], the dipole moments of the initial molecules are higher than those of the corresponding transition states. In elimination of HNO₂ from 3-nitro-1-propene by reaction (2), the dipole moment of

the reactant is somewhat lower than that of the transition state, but the change is so small that it can be neglected (Table 3). Therefore, there are no grounds to apply the conclusions of the Maccoll–Benson theory developed for addition or elimination reactions occurring via a four-membered transition state (which is, indeed, more polar than the initial compounds according to calculations [23]) to β -elimination of HNO₂, occurring via a five-membered transition state.

An interesting feature of HNO₂ elimination from nitroethylene, *trans*-nitropropene, and 2-nitro-1-propene, revealed by descents along reaction pathways from the transition states to the reactants and products [8], should be noted. Namely, processes (2) and (3) yield not infinitely remote alkyne (or alkene) and HNO₂ molecules but complexes of products [R–C≡C–H···HONO] [for reaction (2)] or [R–C(H)=C–R'···HONO] [for reaction (3)] with very weak C···H···C bonds (Figs. 6, 7). These complexes have a lower enthalpy of formation than the final products of the nitroolefin decomposition reactions under consideration (Table 3).

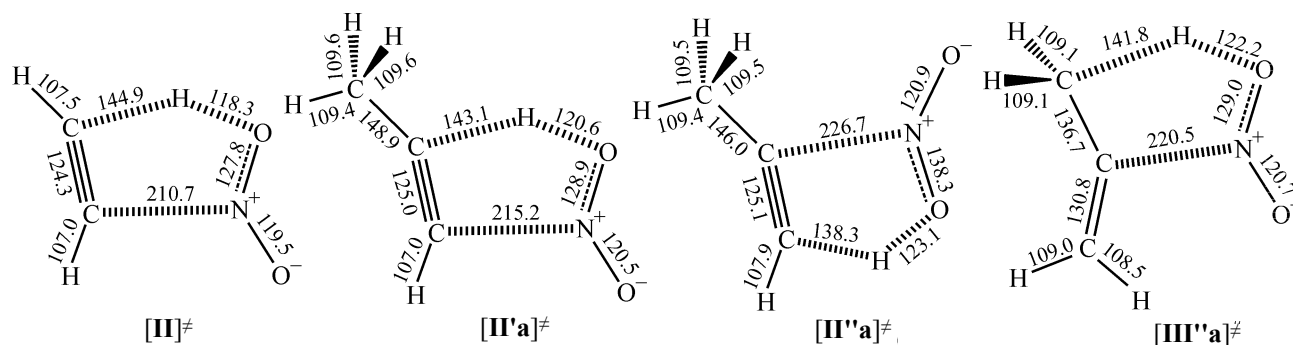


Fig. 4. Geometric parameters of the transition states in HNO₂ elimination from nitroethylene (**[II]‡**), *trans*-nitropropene (**[II'a]‡**), and 2-nitro-1-propene (**[II''a]‡** and **[III'a]‡**), calculated by the B3LYP/6-31G(d) method.

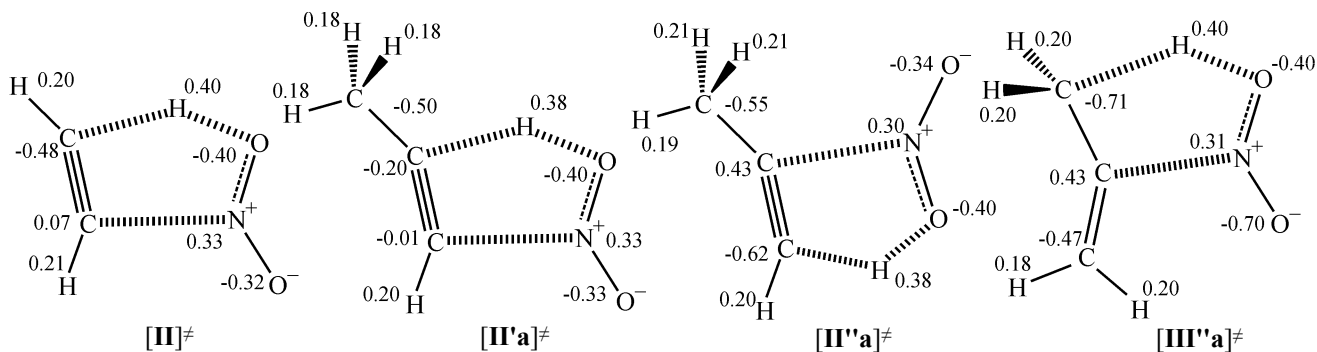


Fig. 5. Charges on atoms (au) of the transition states in HNO₂ elimination from nitroethylene (**[II]‡**), *trans*-nitropropene (**[II'a]‡**), and 2-nitro-1-propene (**[II''a]‡** and **[III'a]‡**), calculated by the B3LYP/6-31G(d) method.

Complexes **II'a** and **II''a** formed from *trans*-nitropropene and 2-nitro-1-propene by HNO_2 elimination from the CH_2 group by reaction (2) contain similar fragments $\text{HC}\equiv\text{C}(\text{CH}_3)$ and HONO , but their mutual orientation is different (Fig. 6). These compounds are characterized by the maximal stabilization relative to the infinitely remote reaction products: $\Delta\Delta H = \Sigma\Delta H_f^{\text{pr}}(298\text{ K}) - \Delta H_f^{\text{c}}(298\text{ K}) = 18.9\text{ kJ mol}^{-1}$ (Table 3). The complex $[\text{HC}=\text{C}=\text{CH}_2\cdots\text{HONO}]$ (**III''a**) formed from 2-nitro-1-propene by hydrogen abstraction from the CH_3 group by reaction (3) is stabilized by 13.5 kJ mol^{-1} , and the complex $[\text{HC}\equiv\text{CH}\cdots\text{HONO}]$ (**II**) formed from nitroethylene has $\Delta\Delta H = 14.2\text{ kJ mol}^{-1}$.

Comparison of the geometric parameters of these compounds (Fig. 6) clearly shows that the most probable cause of a decrease in the stabilization in the series of complexes **II'a** and **II''a**, **II**, and **III''a** is different strength of $\text{C}\cdots\text{H}$ bonds in them. For example, in the first two compounds the $\text{C}\cdots\text{H}$ bonds are appreciably shorter [226.2 and 240.6 pm in complex **II'a**, 228.8 and 237.8 pm in complex **II''a**]

than in the last two compounds [233.1 and 246.7 pm in complex **II**, 246.4 and 237.5 pm in complex **III''a**]. It can be seen that in compound **II'a** one $\text{C}\cdots\text{H}$ bond is longer by 2.8 pm, and the other, shorter by 2.6 pm than in **II''a**. This fact apparently accounts for their equal stabilization relative to the infinitely remote reaction products, propyne and HNO_2 . In complexes **II** and **III''a**, one $\text{C}\cdots\text{H}$ bond has approximately equal length, and the other is shorter by 4.4 pm in the complex of ethyne with HNO_2 than in the complex of propadiene with HNO_2 , which may be responsible for lower $\Delta\Delta H$ for **III''a**.

Nitro–nitrite rearrangement. We showed in [5–8] that the mechanism of the nitro–nitrite rearrangement, which is being actively studied, cannot operate in nitroethylene, because its activation enthalpy exceeds the barrier of the limiting step of 4*H*-1,2-oxazete 2-oxide formation by approximately 30–40 kJ mol^{-1} (Table 1). Nevertheless, examination of this mechanism for substituted nitroolefins is of considerable interest for understanding the general

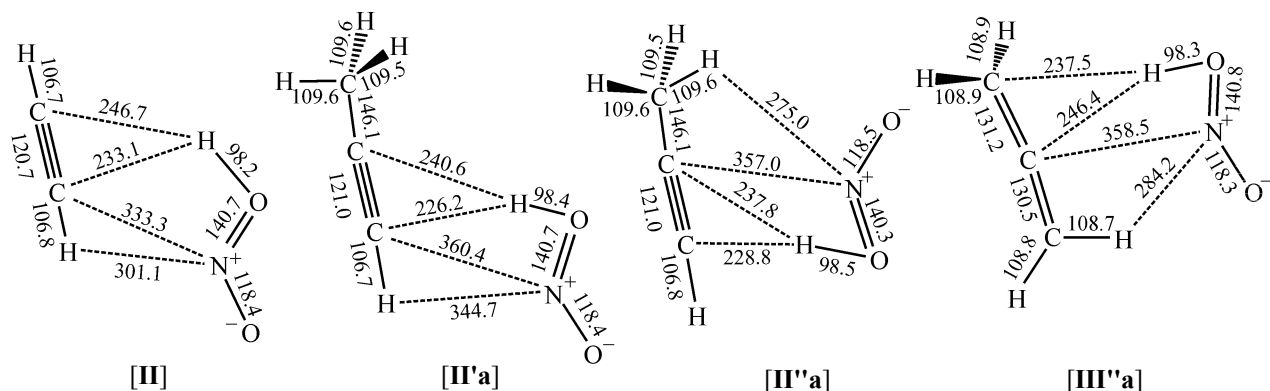


Fig. 6. Geometric parameters of the complexes of products in HNO_2 elimination from nitroethylene (**II**), *trans*-nitropropene (**II'a**), and 2-nitro-1-propene (**II''a** and **III''a**), calculated by the B3LYP/6-31G(d) method.

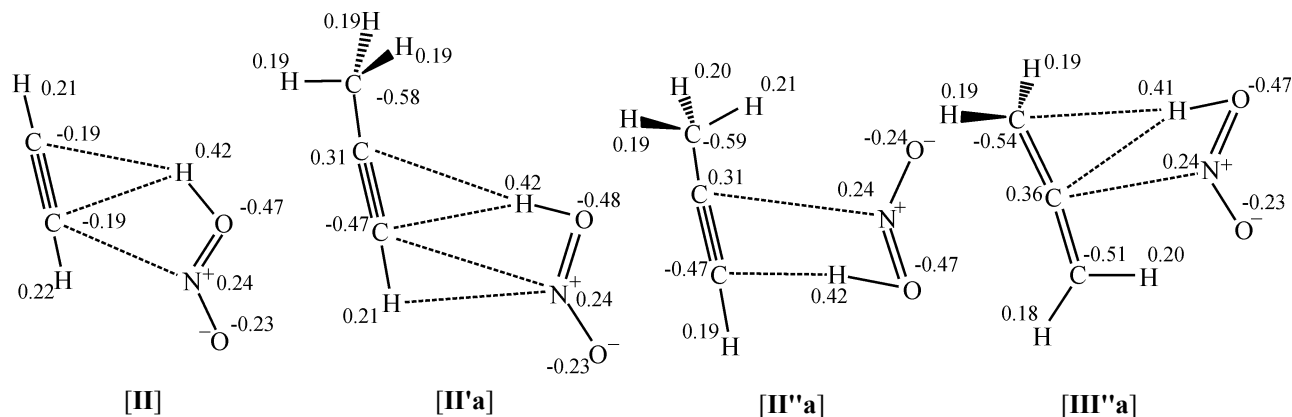


Fig. 7. Charges on atoms (au) of the complexes of products in HNO_2 elimination from nitroethylene (**II**), *trans*-nitropropene (**II'a**), and 2-nitro-1-propene (**II''a** and **III''a**), calculated by the B3LYP/6-31G(d) method.

Table 4. Activation enthalpies ΔH^\ddagger and entropies ΔS^\ddagger , enthalpies of formation of products ΔH_f^{pr} , and dipole moments of reactants, μ_D^0 , transition states, μ_D^\ddagger , and products, μ_D^{pr} , of nitro–nitrite rearrangements of certain nitroolefins

Compound	$\Delta H^\ddagger_{(298\text{ K})}$, kJ mol ^{−1}	$\Delta S^\ddagger_{(298\text{ K})}$, J mol ^{−1} K ^{−1}	$\Delta H_f^{\text{pr}}_{(298\text{ K})}$, kJ mol ^{−1}	μ_D^0	μ_D^\ddagger	μ_D^{pr}
				D		
Nitroethylene	241.5	−1.0	47.4	3.91	2.61	1.63
<i>cis</i> -Nitropropene	240.6	−14.6	22.9	4.31	2.87	1.97
<i>trans</i> -Nitropropene	251.3	−0.3	18.9	4.71	3.22	2.18
2-Nitro-1-propene	233.9	5.8	8.8	3.88	3.26	1.88
2-Methyl-1-nitro-1-propene	239.1	−7.2	−6.8	4.87	3.37	2.32

features of the monomolecular decomposition of C-nitro compounds.

The calculated activation enthalpies and entropies of the process are given in Table 4.

As seen from Table 4, the barriers to nitro–nitrite rearrangement for *trans*-nitropropene are higher by 10 kJ mol^{−1}, and for 2-nitropropene, lower by approximately 8 kJ mol^{−1} than the activation energy of the corresponding reaction with **I**.

This fact cannot be explained from the standpoint of changes in the bond lengths in the course of the reaction (Figs. 2, 8; Table 5), because these changes, e.g., for

trans-nitropropene are smaller, and for 2-nitro-1-propene, considerably larger than for **I**, which should lead to opposite changes in the activation enthalpies for these compounds.

Therefore, the results obtained should be apparently attributed to specific features of charge distribution on atoms of the transition states of the nitro–nitrite rearrangement (Fig. 9). The calculations show that, in the transition states of process (4), the total charges on the nitrogen and oxygen atoms of the reaction center in compounds **I**, **I'****a**, and **I''a** are close, whereas the charges on the C atoms differ significantly. The smallest (nearly zero) charge on

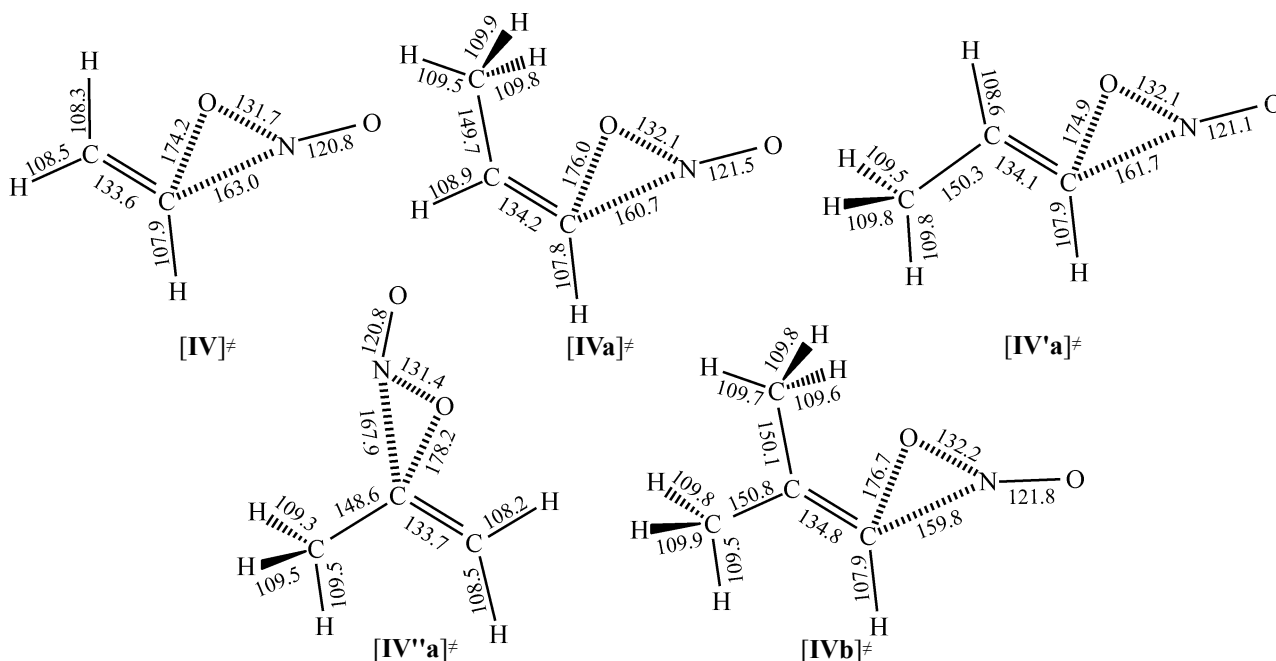
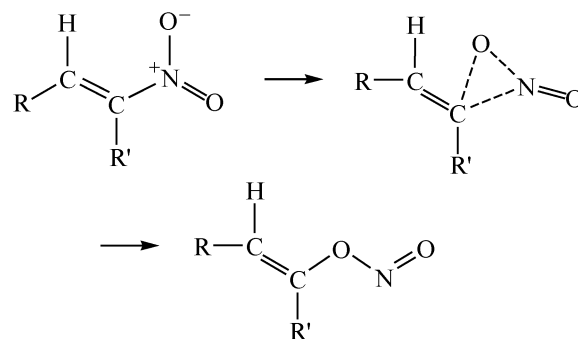
**Fig. 8.** Geometric parameters of the transition states in nitro–nitrite rearrangements of nitroethylene (**[IV]‡**), *cis*-nitropropene (**[IVa]‡**), *trans*-nitropropene (**[IV'a]‡**), 2-nitro-1-propene (**[IV''a]‡**), and 2-methyl-1-nitro-1-propene (**[IVb]‡**), calculated by the B3LYP/6-31G(d) method.

Table 5. Changes Δ in the bond lengths in reaction centers in the course of nitro–nitrite rearrangements (reactant \rightarrow transition state) of certain α -nitroolefins

Compound	Δ CN	Δ CO	Δ NO
	pm		
Nitroethylene	16.5	–58.2	8.8
<i>cis</i> -Nitropropene	15.6	–55.9	8.7
<i>trans</i> -Nitropropene	15.9	–57.4	8.9
2-Nitro-1-propene	19.1	–56.2	8.5
2-Methyl-1-nitro-1-propene	15.2	–55.6	8.6

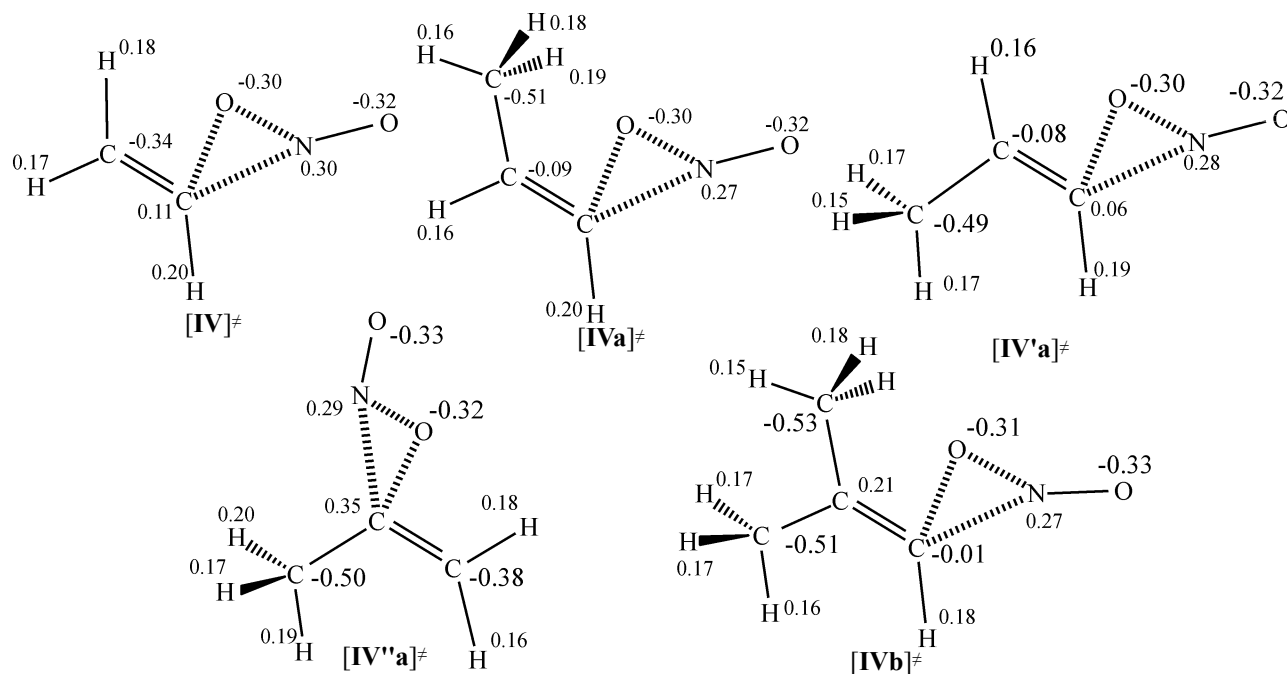
the C atom is obtained for *trans*-nitropropene. For nitroethylene, it is 0.11 au, and for 2-nitro-1-propene, 0.35 au. Obviously, the attraction of the more positively charged carbon atom to the negatively charged oxygen atom will be stronger. This fact stabilizes the transition state and decreases the activation enthalpy of process according to Scheme 4 for **I''a**, compared to the other two compounds under consideration.

For compounds **Ia** and **Ib**, the activation enthalpies

Scheme 4.

of the process are close to those for **I** (Table 4). A slight decrease in the activation enthalpy in the series nitroethylene, *cis*-nitropropene, 2-methyl-1-nitro-1-propene can be accounted for from the standpoint of variation of the geometric parameters in the reaction center (Figs. 2, 8; Table 5). As seen from Table 5, the smallest changes are observed in the reaction center of **Ib**, which accounts for the smallest barrier of the nitro–nitrite rearrangement in this compound compared to the other compounds of the series.

Figures 10 and 11 show the geometric parameters of

**Fig. 9.** Charges on atoms (au) of the transition states in nitro–nitrite rearrangements of nitroethylene (**[IV]‡**), *cis*-nitropropene (**[IVa]‡**), *trans*-nitropropene (**[IV'a]‡**), 2-nitro-1-propene (**[IV''a]‡**), and 2-methyl-1-nitro-1-propene (**[IVb]‡**), calculated by the B3LYP/6-31G(d) method.

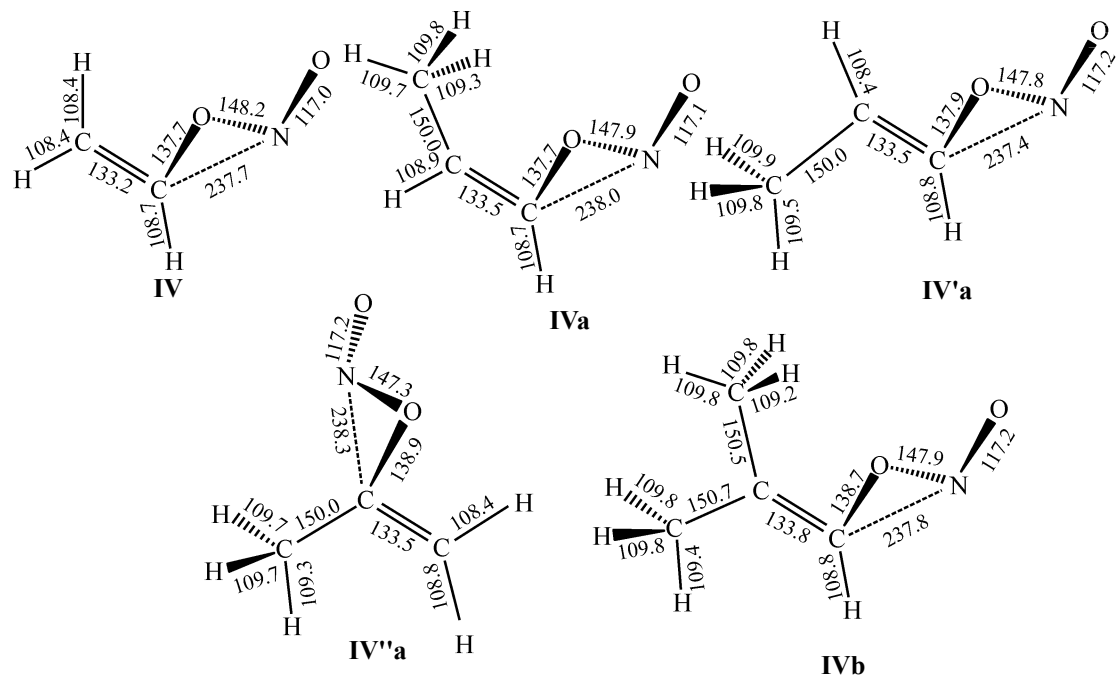


Fig. 10. Geometric parameters of the reaction products in nitro–nitrite rearrangements of nitroethylene (**IV**), *cis*-nitropropene (**IVa**), *trans*-nitropropene (**IV'a**), 2-nitro-1-propene (**IV''a**), and 2-methyl-1-nitro-1-propene (**IVb**), calculated by the B3LYP/6-31G(d) method.

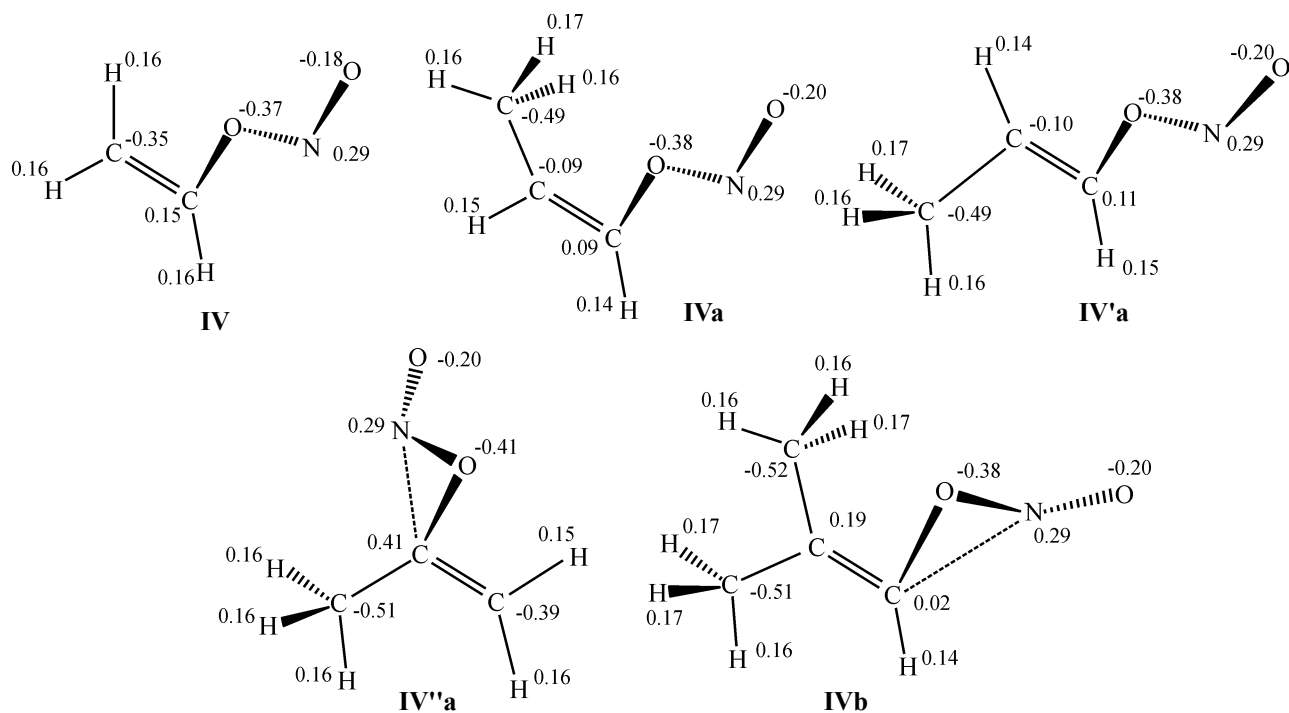


Fig. 11. Charges on atoms (au) of the reaction products in nitro–nitrite rearrangements of nitroethylene (**IV**), *cis*-nitropropene (**IVa**), *trans*-nitropropene (**IV'a**), 2-nitro-1-propene (**IV''a**), and 2-methyl-1-nitro-1-propene (**IVb**), calculated by the B3LYP/6-31G(d) method.

the structures and the charges on atoms (au) of the products of nitro–nitrite rearrangement of all the examined nitroolefins.

1,3-Sigmatropic hydrogen shift with the formation of aci forms. As noted in [24–26], a study of the formation of aci-nitro compounds is of interest for understanding the abnormal instability of dinitromethane and the mechanism of liquid-phase decomposition of nitro compounds. For nitroethylene, we considered previously two alternative processes of formation of aci forms, involving, respectively, 1,3- and 1,4-sigmatropic hydrogen shift to the oxygen atom of the nitro group (Table 1) [5–8].

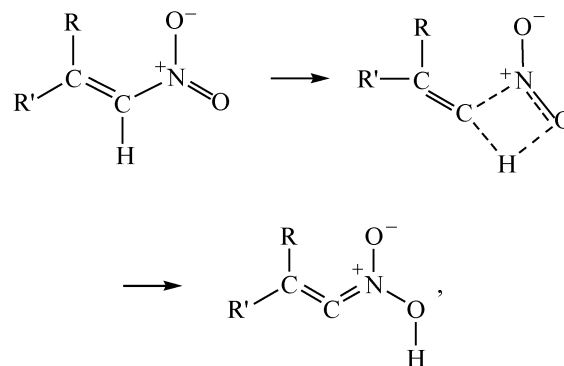
The activation enthalpies of the 1,3-sigmatropic hydrogen shift (Scheme 5) obtained for the four nitroolefins, are given in Table 6.

As can be seen, the reaction barriers for all the examined compounds are close: Their difference is within 2–3 kJ mol^{−1}. At the same time, the activation entropies of the processes differ significantly.

In going from **I** to **I'a**, the activation enthalpy of 1,3-sigmatropic shift of the hydrogen atom somewhat decreases, and the entropy, on the contrary, increases. This change can be readily explained by somewhat more compact transition state for *trans*-nitropropene, compared to nitroethylene (Fig. 12, Table 7).

For **Ia**, the activation enthalpy of the reaction in question is approximately the same as, and the activation entropy, considerably lower than those for **I'a** (Table 6). In this case, changes in the bond lengths in the reaction center in the course of the reaction are still weaker. Substantial decrease in the activation entropy for *cis*-nitropropene can be attributed to strengthening in the transition state of the hydrogen bond (240.2 pm) between the hydrogen atom of the methyl group and the oxygen atom of the nitro group, not involved in the reaction, relative to the initial compound (260.5 pm). In

Scheme 5.



R = R' = H for **I**; R = CH₃, R' = H for **Ia**; R = H, R' = CH₃ for **I'a**; R = R' = CH₃ for **Ib**.

trans-nitropropene this bond, on the contrary, became longer (Figs. 2, 12; Table 7).

For **Ib**, the reaction barrier somewhat decreases, and the activation entropy is intermediate between those for nitroethylene and *cis*-nitropropene (Table 6). A decrease in the activation enthalpy is due to the same factors: more compact transition state in which the changes in the geometric parameters of the reaction center compared to the initial molecule are relatively smaller. At the same time, in the transition state of the 1,3-H shift to the aci form of 2-methyl-1-nitro-1-propene, the hydrogen bond between the hydrogen and oxygen atoms is strengthened relative to the initial compound to a still greater extent, compared to *cis*-nitropropene. This fact is apparently responsible for a decrease in the activation entropy, compared to nitroethylene and *trans*-nitropropene. However, the presence of the second methyl group leads to a relative increase in the activation entropy compared to **Ia** (Figs. 2, 12; Tables 6, 7).

Figure 13 shows the distribution of total electronic

Table 6. Geometric parameters of the complexes of products in HNO₂ elimination from nitroethylene (**II**), *trans*-nitropropene (**II'a**), and 2-nitro-1-propene (**II'a** and **III'a**), calculated by the B3LYP/6-31G(d) method.

Compound	ΔH_f^\ddagger (298 K), kJ mol ^{−1}	ΔS_f^\ddagger (298 K), J mol ^{−1} K ^{−1}	ΔH_f^{pr} (298 K), kJ mol ^{−1}	μ_D^0	μ_D^\ddagger	μ_D^{pr}
				D		
Nitroethylene	257.6	8.1	231.5	3.91	3.92	3.97
<i>cis</i> -Nitropropene	255.3	−14.6	200.5	4.31	3.41	4.36
<i>trans</i> -Nitropropene	255.5	9.9	199.6	4.71	2.33	4.41
2-Methyl-1-nitro-1-propene	252.8	−0.6	169.5	4.87	3.04	4.62

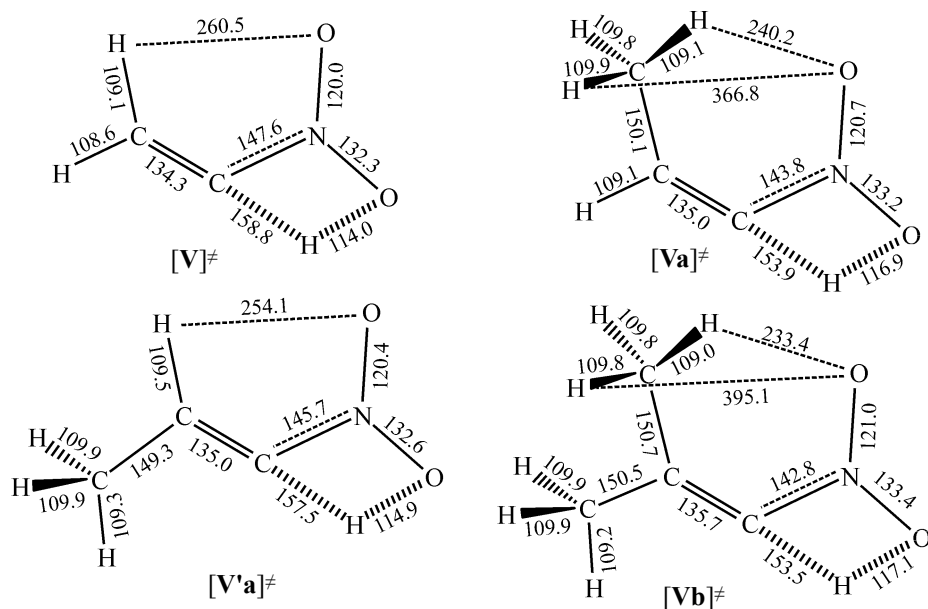


Fig. 12. Geometric parameters of the transition states in 1,3-sigmatropic hydrogen shift to *aci* forms of nitroethylene ($[V]^\ddagger$), *cis*-nitropropene ($[Va]^\ddagger$), *trans*-nitropropene ($[V'a]^\ddagger$), and 2-methyl-1-nitro-1-propene ($[Vb]^\ddagger$), calculated by the B3LYP/6-31G(d) method.

charges on atoms of the transition states in 1,3-sigmatropic hydrogen shift to the *aci* forms of the nitroolefins under consideration, and Figs. 14 and 15 show the structures of the reaction products and the charge distribution in them.

Formation of *aci* forms of nitropropenes via biradicals. Our studies [5–8] of the thermal gas-phase monomolecular decomposition of nitroethylene showed that, for **I**, one more process leading to the formation of the *aci* form is possible, namely, 1,4-sigmatropic hydrogen shift (Scheme 6).

Reaction on Scheme 6 is considerably less favorable energetically than the 1,3-H shift (Table 1), as it occurs via a five-membered biradical transition state (Fig. 16) and is associated with more considerable changes in the

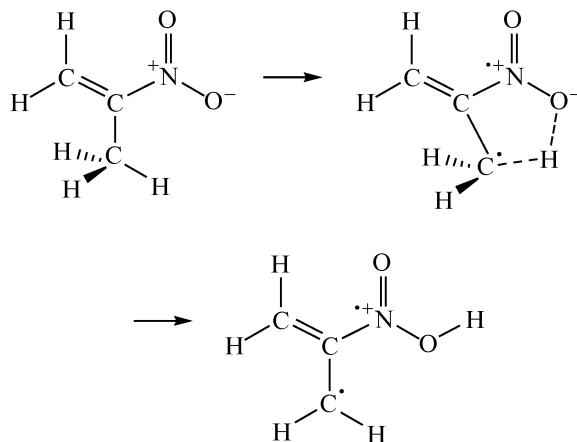
reaction center (Tables 7, 8). Despite this fact, it is of considerable interest for understanding the features of the mechanisms of biradical reactions, playing an important role in thermal decomposition of not only nitroolefins, but also aliphatic nitro compounds as a whole [27, 28]. Nevertheless, this mechanism was not considered for substituted derivatives of **I** because of the high barrier of reaction on Scheme 6.

For 2-nitro-1-propene, hydrogen shift into the *aci* form from the CH_3 group to the oxygen atom of the NO_2 group is possible (Scheme 7).

Table 7. Changes Δ in the bond lengths of reaction centers in the course of 1,3-sigmatropic hydrogen shift to the oxygen atom of the nitro groups with the formation of *aci* forms (reactant \rightarrow transition state) of certain α -nitroolefins

Compound	ΔCN	ΔCH	ΔHO	ΔNO
	pm			
Nitroethylene	1.1	50.6	–126.4	9.2
<i>cis</i> -Nitropropene	–1.3	45.8	–121.8	9.9
<i>trans</i> -Nitropropene	–0.1	49.3	–125.4	9.3
2-Methyl-1-nitro-1-propene	–1.8	45.3	–120.2	9.9

Scheme 6.



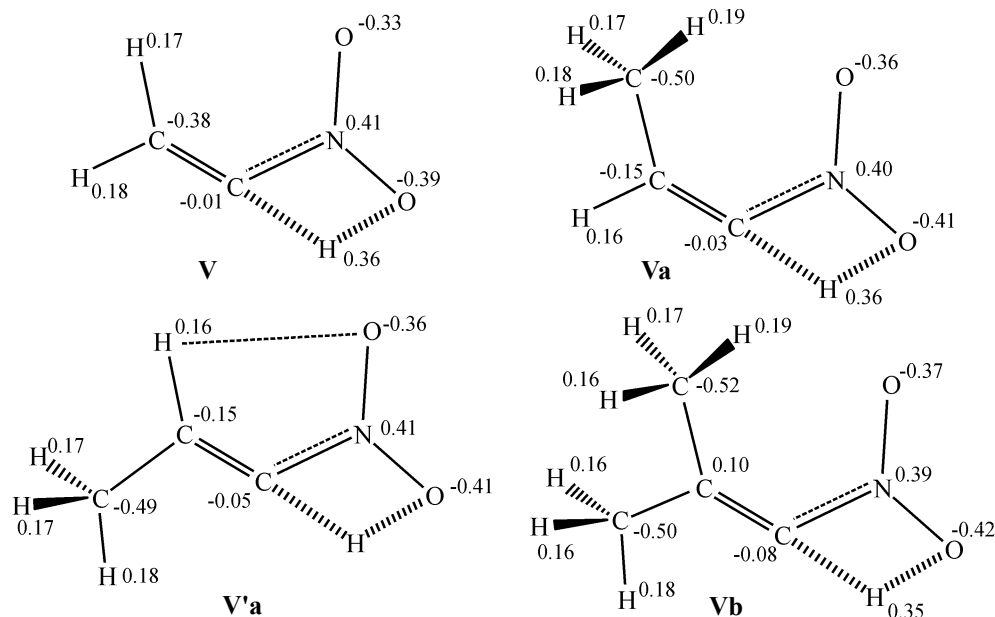


Fig. 13. Charges on atoms (au) of the transition states in 1,3-sigmatropic hydrogen shift to *aci* forms of nitroethylene ($[V]^{\ddagger}$), *cis*-nitropropene ($[Va]^{\ddagger}$), *trans*-nitropropene ($[V'a]^{\ddagger}$), and 2-methyl-1-nitro-1-propene ($[Vb]^{\ddagger}$), calculated by the B3LYP/6-31G(d) method.

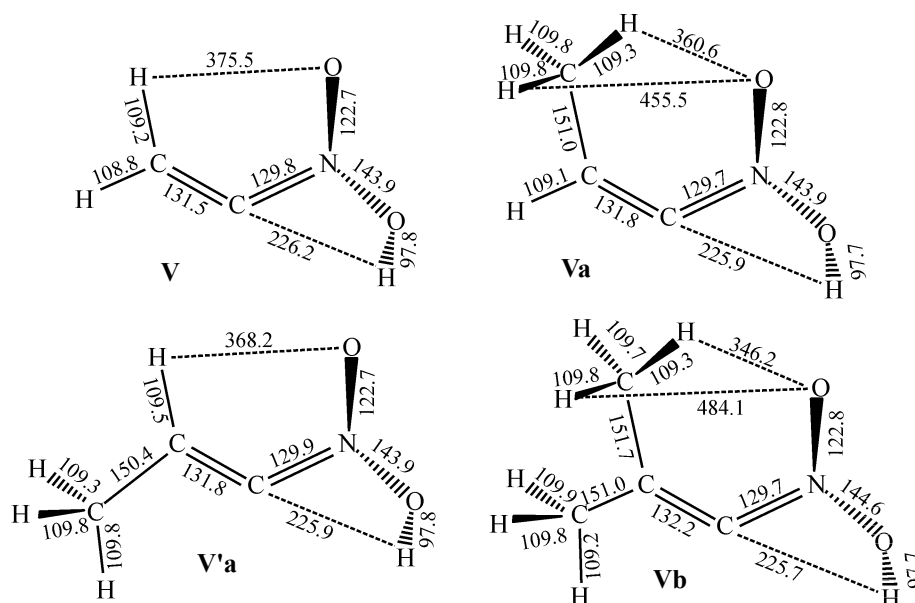


Fig. 14. Geometric parameters of the reaction products in 1,3-sigmatropic hydrogen shift to *aci* forms of nitroethylene (**V**), *cis*-nitropropene (**Va**), *trans*-nitropropene (**V'a**), and 2-methyl-1-nitro-1-propene (**Vb**), calculated by the B3LYP/6-31G(d) method.

The calculated activation enthalpies of reactions (6) and (7) are given in Table 9.

According to Table 9, the activation enthalpy of the transfer of the hydrogen atom from the CH_3 group to the oxygen atom of the NO_2 group of 2-nitro-1-propene is considerably (by approximately 45 kJ mol^{-1}) lower than the energy barrier to 1,4-H shift to the *aci* form

for nitroethylene. This may be due to the fact that reaction (7) involves considerably smaller changes in the geometric parameters than does reaction (6) (Table 8, Fig. 17).

As noted previously, 1,4-sigmatropic hydrogen shift to the *aci* form of nitroethylene occurs via biradical transition state $[VI]^{\ddagger}$ with the formation of biradical

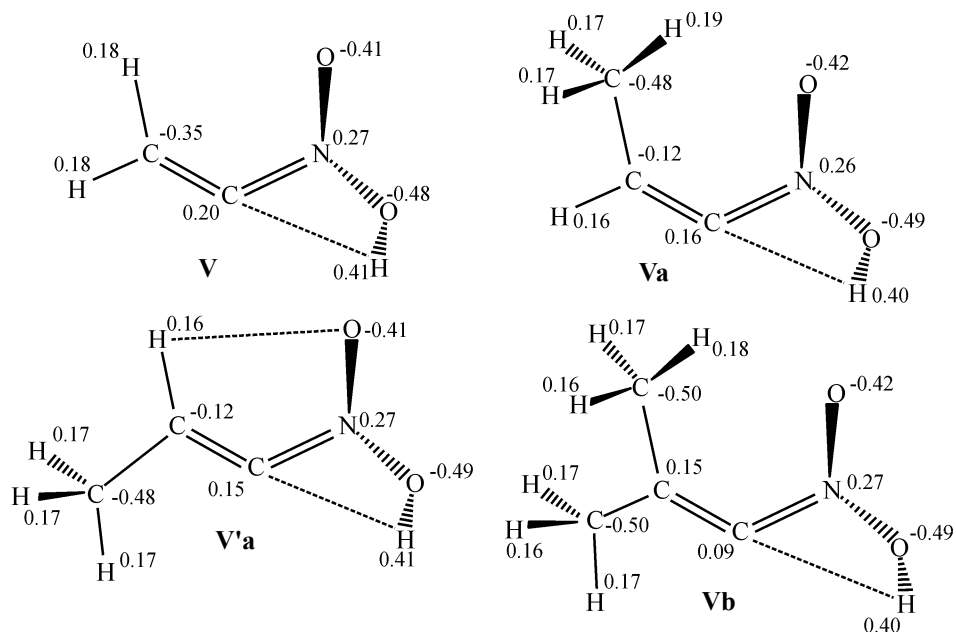


Fig. 15. Charges on atoms (au) of the reaction products in 1,3-sigmatropic hydrogen shift to *aci* forms of nitroethylene (V), *cis*-nitropropene (Va), trans-nitropropene (V'a), and 2-methyl-1-nitro-1-propene (Vb), calculated by the B3LYP/6-31G(d) method.

product VI (Figs. 16, 17). The hydrogen shift to the *aci* form of 2-nitro-1-propene (7) occurs similarly. Possible objections that in both cases zwitterions rather than biradicals are formed are refuted by data on the charge and

spin density distribution (Figs. 3, 16) (the spin density distribution on the reactant atoms is not shown, because it is zero), and also by the dipole moments of the corresponding structures (Table 9). These data demonstrate high degree of spin density polarization on atoms of the reaction centers in transition states [VI][‡], [VII'a][‡] and in compounds VI, VII'a, and also insignificant charge redistribution relative to the initial structures of compounds I and I'a, respectively.

1,5-Sigmatropic hydrogen shift with the formation of *aci* forms. For nitroolefins with a hydrogen-containing substituent in the *cis* position to the nitro group (such as *cis*-nitropropene and 2-methyl-1-nitro-1-propene), one more pathway of the gas-phase decomposition is possible, namely, 1,5-sigmatropic hydrogen shift from the RH group to the nitro group:

Scheme 7.

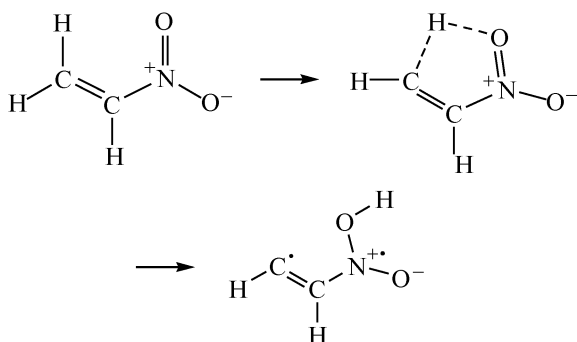


Table 8. Changes Δ in the bond lengths of reaction centers in the course of 1,4-sigmatropic hydrogen shift to the oxygen atom of the nitro groups with the formation of *aci* forms (reactant \rightarrow transition state) of certain α -nitroolefins

Compound	Δ CN	Δ CH	Δ HO	Δ NO	Δ CC
	pm				
Nitroethylene	-5.8	183.1	-147.2	19.5	-2.9
2-Nitro-1-propene	-4.3	66.2	-159.2	11.1	-7.3

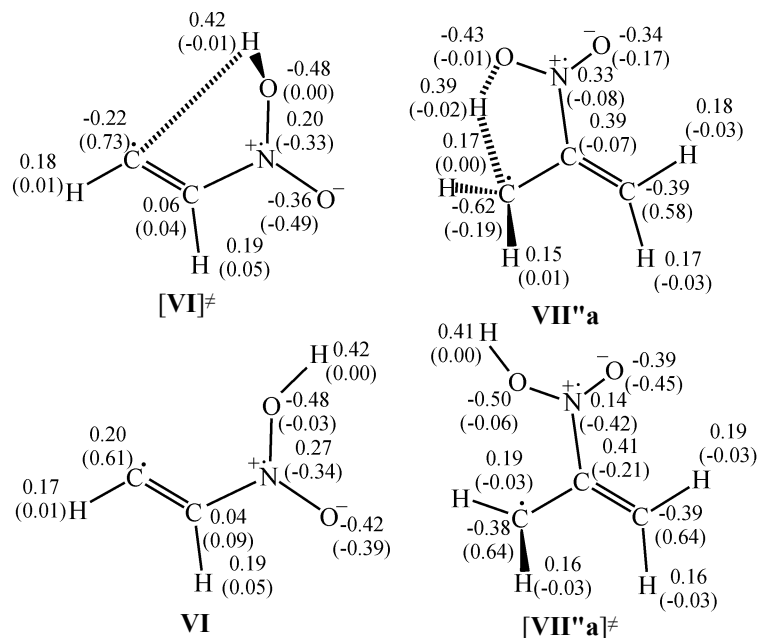


Fig. 16. Charges (spin densities) on atoms (au) of the transition states and products in 1,4-sigmatropic hydrogen shift to *aci* forms of nitroethylene ([VI][‡], VI) and 2-nitro-1-propene ([VII"^a][‡], VII"^a), calculated by the B3LYP/6-31G(d) method.

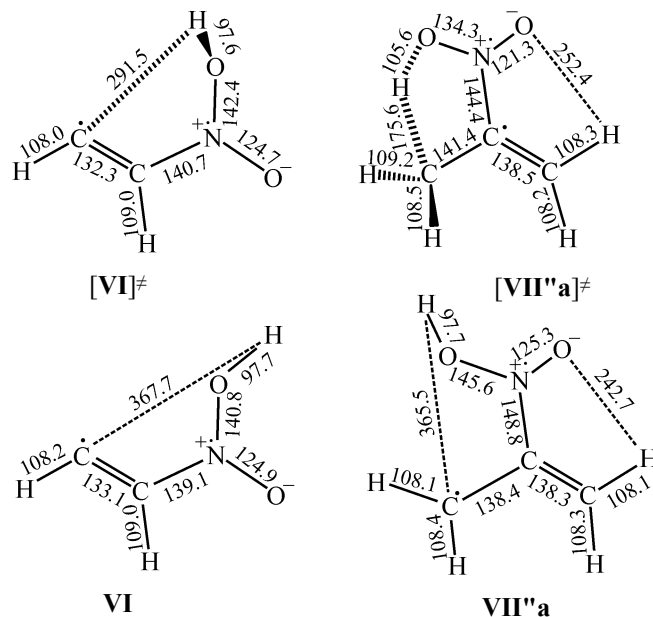


Fig. 17. Geometric parameters of the transition states and products in 1,4-sigmatropic hydrogen shift to *aci* forms of nitroethylene ([VI][‡], VI) and 2-nitro-1-propene ([VII"^a][‡], VII"^a), calculated by the B3LYP/6-31G(d) method.

Table 9. Activation enthalpies ΔH^\ddagger and entropies ΔS^\ddagger , enthalpies of formation of products ΔH_f^{pr} , and dipole moments of the reactants, μ_D^0 , transition states, μ_D^\ddagger , and products, μ_D^{pr} , of 1,4-sigmatropic shift to the *aci* forms of certain nitroolefins

Compound	$\Delta H^\ddagger_{(298\text{ K})}$, kJ mol ⁻¹	$\Delta S^\ddagger_{(298\text{ K})}$, J mol ⁻¹ K ⁻¹	$\Delta H_f^{\text{pr}}_{(298\text{ K})}$, kJ mol ⁻¹	μ_D^0	μ_D^\ddagger	μ_D^{pr}
				D		
Nitroethylene	300.4	8.3	335.3	4.25	3.03	0.81
2-Nitro-1-propene	254.2	-12.4	208.4	3.88	1.55	1.36

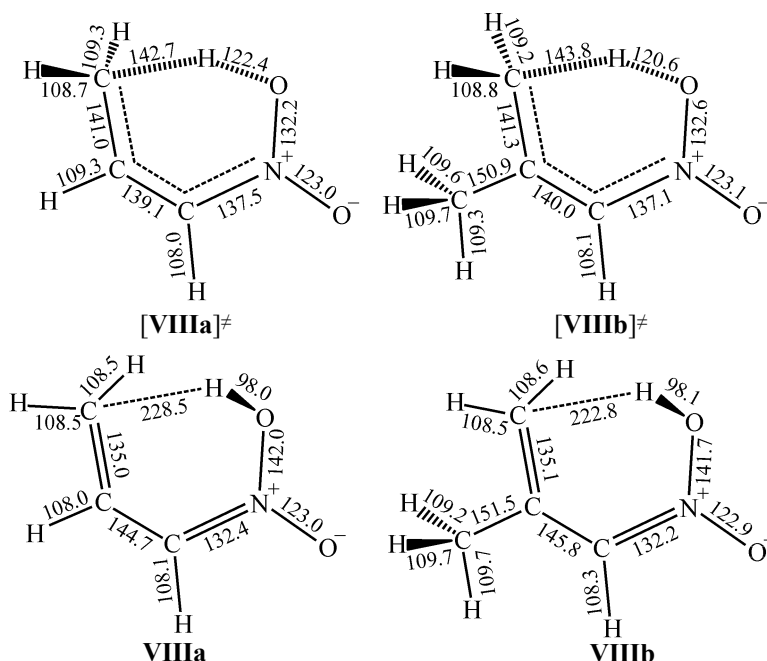
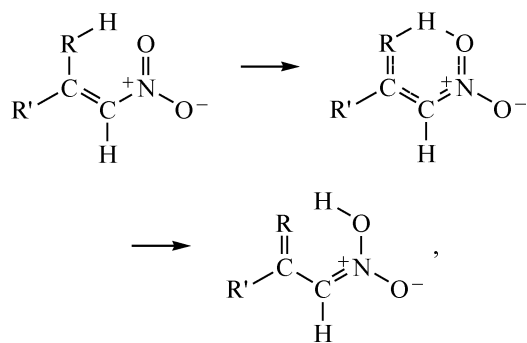


Fig. 18. Geometric parameters of the transition states and products in 1,5-sigmatropic hydrogen shift to *aci* forms of *cis*-nitropropene ([VIIIa][‡], VIIIa) and 2-methyl-1-nitro-1-propene ([VIIIb][‡], VIIIb), calculated by the B3LYP/6-31G(d) method.

Scheme 8.



R = CH₂ and R' = H for **Ia**; R = CH₂ and R' = CH₃ for **Ib**.

The calculated activation enthalpies of process on Scheme 7 are given in Table 10.

The activation enthalpies of the process in question for *cis*-nitropropene and 2-methyl-1-nitro-1-propene are close and are considerably lower than the barriers to the 1,3-sigmatropic shift for the same compounds (Tables 6, 10).

Close activation enthalpies of the 1,5-H shift to the *aci* forms of *cis*-nitropropene and 2-methyl-1-nitro-1-propene indicate that the second methyl group in **Ib** does not affect the reaction course.

A considerable decrease in the activation enthalpy of reaction (8), compared to the previously described reaction (5), can be attributed to several factors, namely:

(i) in the course of 1,3- and 1,5-H shifts to the *aci*

Table 10. Activation enthalpies ΔH^\ddagger and entropies ΔS^\ddagger , enthalpies of formation of products ΔH_f^{pr} , and dipole moments of the reactants, μ_D^0 , transition states, μ_D^\ddagger , and products, μ_D^{pr} , of 1,5-sigmatropic shift to the *aci* forms of certain nitroolefins

Compound	$\Delta H^\ddagger_{(298\text{ K})}$, kJ mol ⁻¹	$\Delta S^\ddagger_{(298\text{ K})}$, J mol ⁻¹ K ⁻¹	$\Delta H_f^{\text{pr}}_{(298\text{ K})}$, kJ mol ⁻¹	μ_D^0	μ_D^\ddagger	μ_D^{pr}
				D		
<i>cis</i> -Nitroethylene	140.7 (176.6) ^a	-38.4	105.6	4.31	3.78	3.94
2-Methyl-1-nitro-1-propene	139.8	-22.7	79.2	4.87	4.39	4.29

^a Results of MP2/6-31G(d) calculations [29].

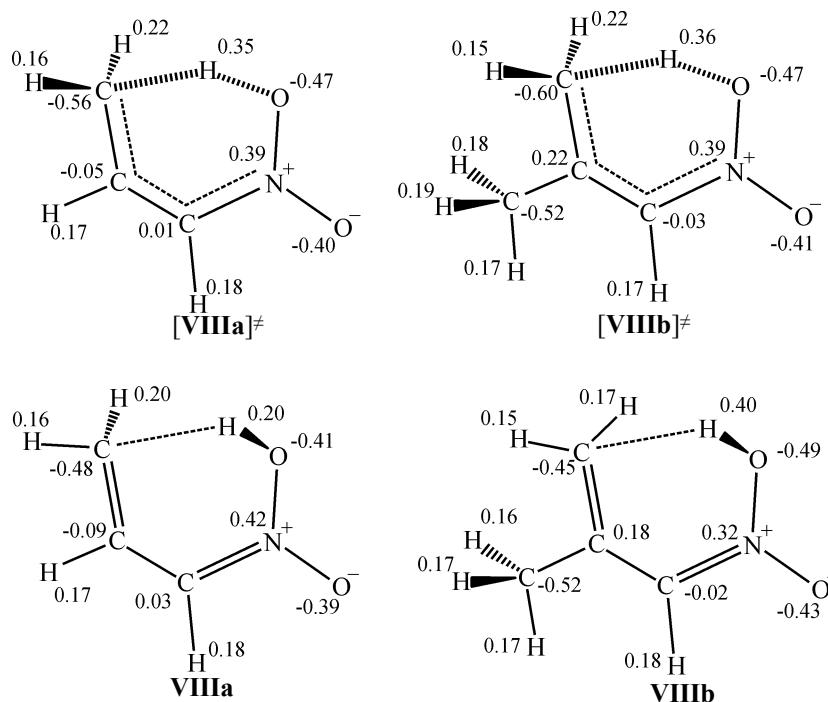


Fig. 19. Charges on atoms (au) of the transition states and products in 1,5-sigmatropic hydrogen shift to *aci* forms of *cis*-nitropropene ([VIIIa][‡], VIIIa) and 2-methyl-1-nitro-1-propene ([VIIIb][‡], VIIIb), calculated by the B3LYP/6-31G(d) method.

forms, the CH, NO, and CN bonds undergo the strongest changes (Figs. 2, 12, 18; Tables 7, 11). Whereas in reaction (5) the CH bond that undergoes cleavage is elongated by approximately 45–46 pm, in reaction (8) the elongation is smaller: 33–34 pm. Such changes are attributable to higher strength and lower polarity of the CH bond at the CC double bond, compared to the CH bond in the methyl group at the CC single bond (Figs. 2, 3);

(ii) reaction (8) leads to the formation of two double bonds CC and CN, whereas in reaction (5) only one CN bond is strengthened;

(iii) 1,5-sigmatropic hydrogen shift leads to the formation of more stable *aci* forms of the examined nitroolefins than does reaction (5), as indicated by the enthalpies of formation of the reaction products (Tables 6, 10).

Figures 18 and 19 show the geometric structures of

reaction products and the atomic charge distribution in the transition states and products of the 1,5-sigmatropic hydrogen shift with the formation of the *aci* forms of *cis*-nitropropene and 2-methyl-1-nitro-1-propene.

Formation of substituted oxazetes. As already noted, the mechanism of the monomolecular gas-phase decomposition of nitroethylene involves formation in the limiting step of a cyclic intermediate, 4*H*-1,2-oxazete 2-oxide [9]. It was interesting to examine the possibility of realization of the cyclization pathway for nitropropenes.

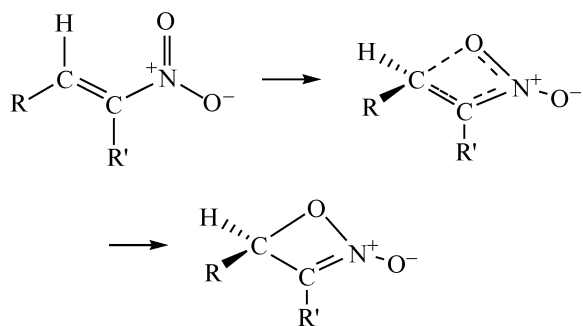
The calculated activation enthalpies of the primary event of the cyclization mechanism for five nitroolefins (Scheme 9) are given in Table 12.

Table 12 shows that introduction of the methyl group into the α -position to the nitro group in *cis*- and *trans*-nitropropenes leads to a decrease by approximately 4 and

Table 11. Changes Δ in the bond lengths of reaction centers in the course of 1,5-sigmatropic hydrogen shift to the oxygen atom of the nitro groups with the formation of *aci* forms (reactant \rightarrow transition state) of certain α -nitroolefins

Compound	Δ CN	Δ CH	Δ HO	Δ NO	Δ CC	Δ C–C _{CH}
	pm					
<i>cis</i> -Nitropropene	–7.6	33.3	–138.6	9.0	5.2	–9.0
2-Methyl-1-nitro-1-propene	–7.5	34.3	–134.3	9.0	5.5	–9.4

Scheme 9.



15 kJ mol⁻¹, respectively, in the barriers to formation of cyclic intermediates (substituted oxazetes) relative to nitroethylene. This fact can be attributed to weakening of the repulsion between the C¹ and O⁴ atoms (Fig. 3) in *cis*- and *trans*-nitropropenes compared to nitroethylene owing to a decrease in the negative charge on the C¹ atoms in compounds **Ia** and **I'a** (−0.07 au) relative to **I** (−0.31 au), whereas the charge on the O⁴ atom in all the three compounds is essentially the same.

For the *cis* isomer of nitropropene, the activation enthalpy of the formation of 4-methyl-4*H*-1,2-oxazete 2-oxide (**IXa**) is higher by approximately 11 kJ mol⁻¹ than for the *trans* isomer (Table 12). This fact cannot be rationalized from the standpoint of the variation of charges on atoms of the reaction center of the initial compounds, because the charge distribution on the C¹, C², N³, and O⁴ atoms in *cis*- and *trans*-nitropropenes is similar (Fig. 3). However, for **Ia** one can expect relatively strong repulsion of the oxygen atom of the nitro group (O⁴) from the methyl carbon atom (C⁷), as both bear significant negative charges, and also the steric repulsion of the CH₃ and NO₂ fragments. This is confirmed by data on the total charge distribution on the reactant atoms (Fig. 3) and on the structures of the reactants, transition states, and products

of the process (Figs. 2, 20, 21; Table 12). As seen from Figs. 2, 20, and 21 and from Table 12, cyclization of the *trans* isomer involves considerably smaller changes in the C¹O⁴ bond length and bond angles than does the cyclization of *cis*-nitropropene.

For 2-nitro-1-propene, the activation enthalpy of the formation of 3-methyl-4*H*-1,2-oxazete 2-oxide (**IX''a**) is virtually equal to the barrier to cyclization of **Ia**. Consideration of the charge distribution on atoms of the initial compounds (Fig. 3) shows that the negative charge on the C¹ atom in **I''a** (−0.36 au) increases relative to nitroethylene (−0.31 au) and *trans*-nitropropene (−0.07 au). According to this data, one might expect an increase in the barrier to cyclization of 2-nitro-1-propene relative to **I** and **I'a**. Relative to *trans*-nitropropene, this is the case. However, as seen from Table 12, relative to nitroethylene the pattern is opposite. At the same time, the bond lengths in the transition states [**IX''a**][‡], [**IX**][‡], and [**IX'a**][‡] are close (Fig. 20).

The presence in **I''a** of a bulkier substituent (R = CH₃) at the carbon atom bound to the nitro group, compared to **I** (R = H), suggest the occurrence of steric strains in 2-nitro-1-propene. Indeed, comparison of the RCN bond angles in the reactants of the cyclization process shows that, in **I''a**, this angle is somewhat larger (∠CH₃–CN = 114.8°) than in **I** (∠HCN = 111.9°) (Fig. 2). Owing to an increase in the RCN angle, the distance between the O and C atoms forming the bond in the course of cyclization appreciably decreases (by almost 5 pm) in 2-nitro-1-propene compared to nitroethylene. At the same time, as already noted, the geometric parameters of the reaction center in both compounds are similar (Fig. 20). Hence, decreased barrier to formation of 3-methyl-4*H*-1,2-oxazete 2-oxide (**IX''a**) from **I''a**, relative to the formation of 4*H*-1,2-oxazete 2-oxide from **I**, is apparently caused by smaller required structural rearrangements in the course

Table 12. Activation enthalpies ΔH^\ddagger and entropies ΔS^\ddagger , enthalpies of formation of products ΔH_f^{pr} , and dipole moments of the reactants, μ_D^0 , transition states, μ_D^\ddagger , and products, μ_D^{pr} , of cyclization of certain nitroolefins into oxazetes

Compound	$\Delta H^\ddagger_{(298\text{ K})}$, kJ mol ⁻¹	$\Delta S^\ddagger_{(298\text{ K})}$, J mol ⁻¹ K ⁻¹	$\Delta H_f^{\text{pr}}_{(298\text{ K})}$, kJ mol ⁻¹	μ_D^0	μ_D^\ddagger	μ_D^{pr}
				D		
Nitroethylene	201.3	−13.1	127.9	3.91	4.27	3.82
<i>cis</i> -Nitropropene	197.3	−32.5	92.0	4.31	4.76	4.01
<i>trans</i> -Nitropropene	186.8	−8.2	92.0	4.71	5.12	4.01
2-Nitro-1-propene	196.7	−3.8	84.3	3.88	4.51	4.26
2-Methyl-1-nitro-1-propene	182.2	−19.8	60.8	4.87	5.46	4.14

of the reaction (Table 13), which, in turn, is due to steric interaction of the functional groups CH_3 and NO_2 .

Introduction of the second methyl group into the α -position to the nitro group in 2-methyl-1-nitro-1-propene

leads to a decrease by approximately 18 kJ mol^{-1} in the barrier to formation of the cyclic intermediate, compared to the activation enthalpy of the related reaction in *cis*-nitropropene. The decrease in the barrier to cyclization

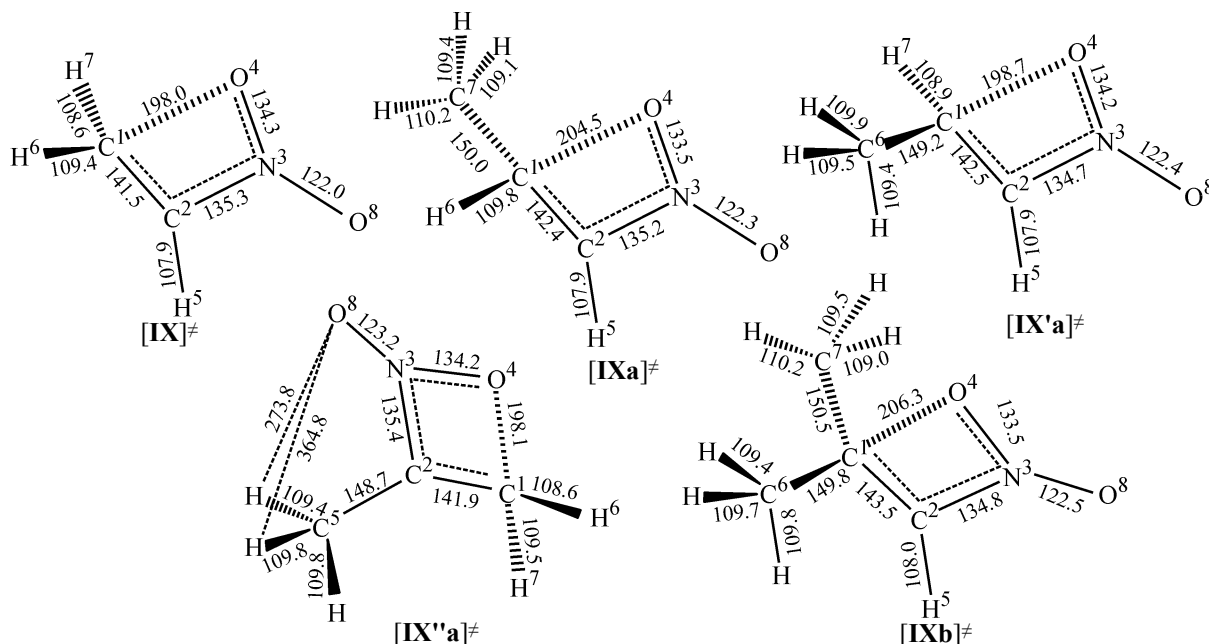


Fig. 20. Geometric parameters of the transition states in cyclization of nitroethylene ($[\text{IX}]^\ddagger$), *cis*-nitropropene ($[\text{IXa}]^\ddagger$), *trans*-nitropropene ($[\text{IX'a}]^\ddagger$), 2-nitro-1-propene ($[\text{IX''a}]^\ddagger$), and 2-methyl-1-nitro-1-propene ($[\text{IXb}]^\ddagger$), calculated by the B3LYP/6-31G(d) method.

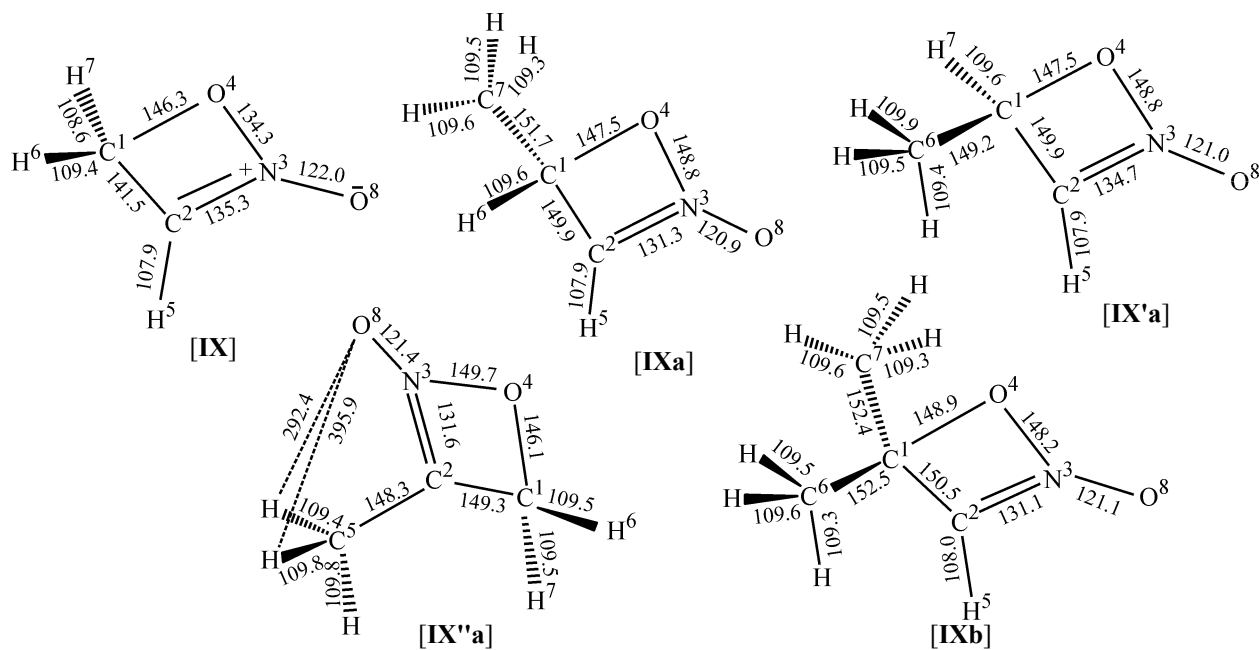


Fig. 21. Geometric parameters of the reaction products in cyclization of nitroethylene (**IX**), *cis*-nitropropene (**IXa**), *trans*-nitropropene (**IX'a**), 2-nitro-1-propene (**IX''a**), and 2-methyl-1-nitro-1-propene (**IXb**), calculated by the B3LYP/6-31G(d) method.

Table 13. Changes in the bond lengths Δ and in the bond angles $\Delta\angle$ in the reaction center in the course of cyclization of certain α -nitroolefins (reactant \rightarrow transition state)

Compound	ΔC^1C^2	ΔC^2N^3	ΔN^3O^4	ΔO^4C^1	$\Delta\angle C^1C^2N^3$	$\Delta\angle C^2N^3O^4$	$\Delta\angle N^3O^4C^1$	$\Delta\angle O^4C^1C^2$
	pm				deg			
Nitroethylene	6.3	-11.2	11.4	-76.3	-20.0	-14.2	14.9	18.1
<i>cis</i> -Nitropropene	8.5	-9.9	10.1	-81.2	-22.7	-13.6	16.0	20.0
<i>trans</i> -Nitropropene	9.2	-11.1	11.0	-76.2	-19.8	-14.3	15.3	17.8
2-Nitro-1-propene	8.7	-13.4	11.3	-71.5	-17.2	-13.6	13.6	15.8
2-Methyl-1-nitro-1-propene	9.0	-9.8	9.7	-77.6	-22.3	-13.3	15.8	19.2

of **Ib** relative to the reactions of *cis*- and *trans*-nitropropenes can be rationalized by analyzing the atomic charge distribution in these molecules (Fig. 3).

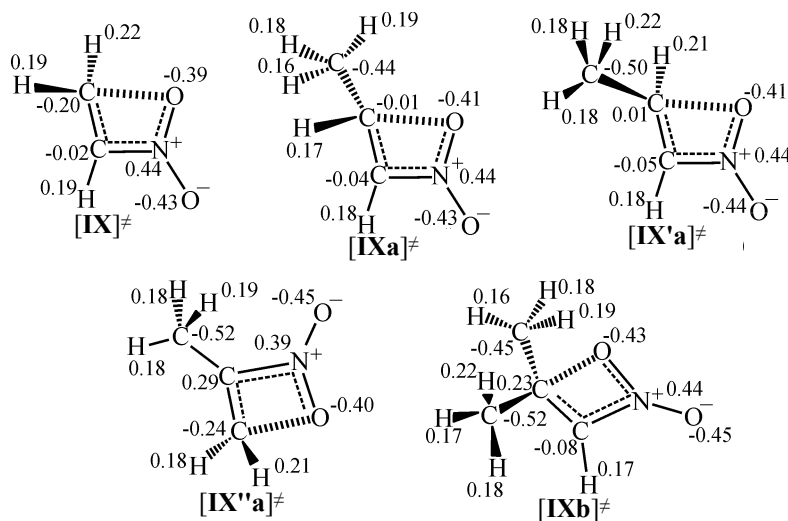
As seen from Fig. 3, in nitroethylene the C^1 atom bears a significant (-0.31 au) negative charge. In *cis*- and *trans*-nitropropenes, the methyl group only weakly polarizes the C^1C^2 bond, and a slight negative charge (-0.07 au) is preserved on the second carbon atom. On the contrary, the second CH_3 group appearing in 2-methyl-1-nitro-1-propene strongly polarizes this bond, and a positive charge (0.20 au) appears on C^1 . The charge on the O^4 atom participating in the formation of the cyclic intermediate is approximately equal in all the four compounds (~ 0.4 au). This may lead to a decreased cyclization barrier compared to the reactions of nitroethylene and *cis*- and *trans*-nitropropenes.

Figures 22 and 23 show the distribution of the total electronic charges on atoms of the transition states and

reaction products in formation of substituted oxazetes from the nitroolefins under consideration.

CONCLUSIONS

(1) The results of a quantum-chemical study of alternative mechanisms of gas-phase monomolecular thermal decomposition of isomeric and substituted nitropropenes, performed by the B3LYP/6-31G(d) hybrid method of the density functional theory, show that possible mechanisms of thermal degradation of *trans*-nitropropene and 2-nitro-1-propene involve formation in the primary steps of 4-methyl-4*H*-1,2-oxazete 2-oxide and 3-methyl-4*H*-1,2-oxazete 2-oxide, respectively. For *cis*-nitropropene and 2-methyl-1-nitro-1-propene, the decomposition pathways involving 1,5-sigmatropic hydrogen shift from the hydrogen-containing substituent to the oxygen atom

**Fig. 22.** Charges on atoms (au) of the transition states in cyclization of nitroethylene ($[IX]^{\ddagger}$), *cis*-nitropropene ($[IXa]^{\ddagger}$), *trans*-nitropropene ($[IX'a]^{\ddagger}$), 2-nitro-1-propene ($[IX''a]^{\ddagger}$), and 2-methyl-1-nitro-1-propene ($[IXb]^{\ddagger}$), calculated by the B3LYP/6-31G(d) method.

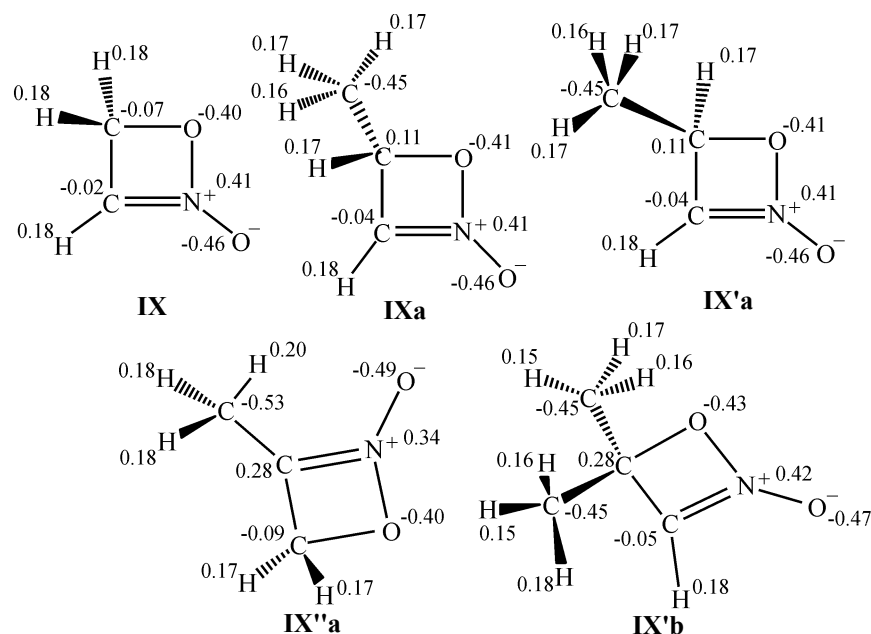


Fig. 23. Charges on atoms (au) of 4*H*-1,2-oxazete 2-oxide (**IX**), 2-methyl-4*H*-1,2-oxazete 2-oxide (**IXa**, **IX'a**), 3-methyl-4*H*-1,2-oxazete 2-oxide (**IX''a**), and 4,4-dimethyl-4*H*-1,2-oxazete 2-oxide (**IX'b**), calculated by the B3LYP/6-31G(d) method.

of the NO₂ group are preferable.

(2) In the mechanism of the 1,5-H shift to the *aci* form for *cis*-nitropropene and 2-methyl-1-nitro-1-propene, which is of considerable interest, the limiting step is not the primary event, formation of the *aci* forms, but their transformation via a series of conformational transitions into isoxazol-2(5*H*)-ol or 4-methylisoxazol-2(5*H*)-ol.

The relative enthalpies of formation of the transition states are 182.5 and 190.0 kJ mol⁻¹, respectively.

(3) The mechanisms of gas-phase monomolecular decomposition of *cis*-nitropropene and 2-methyl-1-nitro-1-propene, involving the formation of 4-methyl-4*H*-1,2-oxazete 2-oxide and 4,4-dimethyl-4*H*-1,2-oxazete 2-oxide, respectively, cannot be fully ruled out. The probability of the occurrence of this mechanism is significantly higher for 2-methyl-1-nitro-1-propene.

(4) The possibility of competition of two alternative mechanisms of thermal decomposition, with cyclization to oxazetes and 1,5-sigmatropic hydrogen shift to the oxygen atom of the nitro group as primary events, is demonstrated.

REFERENCES

1. Politzer, P., Concha, M.C., Grice, M.E., et al., *J. Mol. Struct. (THEOCHEM)*, 1998, vol. 452, p. 75.
2. Latypov, N.V., Bergman, J., Langlet, A., et al., *Tetrahedron*, 1998, vol. 54, p. 11525.
3. Östmark, H., Langlet, A., Bergman, H., et al., in *11th Int. Symp. on Detonation*, 1998 [http://www.saince.com/ear/detsymp/financemt.html].
4. Gindulyte, A., Massa, L., Huang, L., and Karle, J., *J. Phys. Chem. A*, 1999, vol. 103, p. 11045.
5. Shamov, A.G. and Khrapkovskii, G.M., Abstracts of Papers, *30th Int. Annual Conf. of ICT, Karlsruhe*, 1999, p. 60-1.
6. Shamov, A.G. and Khrapkovskii, G.M., in *Struktura i dinamika molekulyarnykh sistem* (Structure and Dynamics of Molecular Systems), Kazan, 1999, issue 6.
7. Shamov, A.G. and Khrapkovskii, G.M., *Mendeleev Commun.*, 2001, no. 4, p. 163.
8. Shamov, A.G., Nikolaeva, E.V., and Khrapkovskii, G.M., *Zh. Obshch. Khim.*, 2004, vol. 74, no. 8, p. 1327.
9. Nazin, G.M. and Manelis, G.B., *Usp. Khim.*, 1994, vol. 63, no. 4, p. 327.
10. Kinstle, T.H. and Stam, J.G., *J. Org. Chem.*, 1970, vol. 35, no. 6, p. 1771.
11. Wieser, K. and Berndt, A., *Angew. Chem.*, 1975, vol. 87, no. 2, p. 72.
12. Wieser, K. and Berndt, A., *Angew. Chem.*, 1975, vol. 87, no. 2, p. 73.
13. Egsgaard, H. and Carlsen, L., *Org. Mass Spectrom.*, 1989, vol. 24, p. 1031.
14. Frisch, M.J., Trucks, G.W., Schlegel, H.B., et al., *Gaussian*

- 98 (Revision A.1), Pittsburgh PA: Gaussian, 1998.
15. Aminova, R.M., Glagolev, A.A., and Shamov, A.G., in *Struktura i dinamika molekulyarnykh sistem* (Structure and Dynamics of Molecular Systems), Ioshkar-Ola, 2005, issue 12, part 1, p. 12.
 16. Khrapkovskii, G.M., Chachkov, D.V., and Shamov, A.G., *Zh. Obshch. Khim.*, 2001, vol. 71, no. 9, p. 1530.
 17. Khrapkovskii, G.M., Nikolaeva, E.V., Chachkov, D.V., et al., in *Struktura i dinamika molekulyarnykh sistem* (Structure and Dynamics of Molecular Systems), Ioshkar-Ola, 2001, issue 8, part 2, p. 202.
 18. NIST Standard Reference Database [<http://webbook.nist.gov/chemistry>].
 19. Turner, A.G., *J. Phys. Chem.*, 1986, vol. 90, p. 6000.
 20. Nazin, G.M., Manelis, G.B., and Dubovitskii, F.I., *Usp. Khim.*, 1968, vol. 37, no. 8, p. 1443.
 21. Manelis, G.B., Nazin, G.M., Rubtsov, Yu.I., and Strunin, V.A., *Termicheskoe razlozhenie i gorenie vzryvchatykh veshchestv i porokhov* (Thermal Decomposition and Combustion of Explosives and Gunpowders), Moscow: Nauka, 1996.
 22. Dubikhin, V.V., Nazin, G.M., and Manelis, G.B., *Izv. Akad. Nauk SSSR, Ser. Khim.*, 1974, no. 6, p. 1345.
 23. Khrapkovskii, G.M., Marchenko, G.N., and Shamov, A.G., *Vliyaniye molekulyarnoi struktury na kineticheskie parametry monomolekulyarnogo raspada C- i O-nitrosoedinenii* (Influence of Molecular Structure on Kinetic Parameters of Monomolecular Decomposition of C- and O-Nitro Compounds), Kazan: FEN, 1997.
 24. Shamov, A.G., Khrapkovskii, G.M., and Shamov, G.A., in *Struktura i dinamika molekulyarnykh sistem* (Structure and Dynamics of Molecular Systems), Ioshkar-Ola, 1998, issue 5, p. 85.
 25. Dewar, M.J.S., Ritchie, J.P., and Alster, J., *J. Org. Chem.*, 1985, vol. 50, p. 1031.
 26. Khrapkovskii, G.M., Shamov, A.G., Shamov, G.A., and Slyapochnikov, V.A., *Mendeleev Commun.*, 1997, no. 5, p. 169.
 27. Nikolaeva, E.V., Shamov, A.G., Chachkov, D.V., and Khrapkovskii, G.M., in *Struktura i dinamika molekulyarnykh sistem* (Structure and Dynamics of Molecular Systems), Kazan, 2003, issue 10, part 3, p. 241.
 28. Shamov, A.G., Nikolaeva, E.V., Chachkov, D.V., and Khrapkovskii, G.M., Abstracts of Papers, *35th Int. Annual Conf. of ICT, Karlsruhe*, 2004, p. 127-1.